

University of Alberta

Effect of fluidization on adsorption of volatile organic
compounds on beaded activated carbon

by

Samineh Kamravaei

A thesis submitted to the Faculty of Graduate Studies and Research in
partial fulfillment of the requirements for the degree of

Master of Science

in

Environmental Engineering

Civil and Environmental Engineering

© Samineh Kamravaei

Spring 2014

Edmonton, Alberta

Permission is hereby granted to the University of Alberta Libraries to reproduce single copies of this thesis and to lend or sell such copies for private, scholarly or scientific research purposes only. Where the thesis is converted to, or otherwise made available in digital form, the University of Alberta will advise potential users of the thesis of these terms.

The author reserves all other publication and other rights in association with the copyright in the thesis and, except as herein before provided, neither the thesis nor any substantial portion thereof may be printed or otherwise reproduced in any material form whatsoever without the author's prior written permission.

DEDICATION

I would like to dedicate this thesis to my lovely parents that this success could not be achieved without your endless love, encouragement and support.

ABSTRACT

Adsorption on activated carbon is a widely used technique for controlling emissions of volatile organic compounds (VOCs) from automotive painting booths; however, irreversible adsorption is a common challenge in this process. This research investigates the effect of adsorbent bed configuration on adsorption of VOCs on beaded activated carbon (BAC). Fixed and fluidized bed adsorption of a single compound (1, 2, 4 – trimethylbenzene) and a mixture of nine organic compounds representing different organic groups were accomplished in five consecutive cycles. Adsorption tests were completed either in partial or full loading of the adsorbent. All regeneration cycles were completed in fixed bed arrangement. The results demonstrated similar adsorption capacities obtained in both configurations. However, 30 – 42% lower heel formation was found using fluidized bed than in fixed bed in case of the VOCs mixture. Thermo – gravimetric analysis confirmed less organic accumulation on BAC after regeneration for the bed loaded with the VOCs mixture in fluidized bed configuration. The lower irreversible adsorption obtained using fluidized bed adsorption could be due to improved mass transfer and more complete utilization of BAC's available pore volume in the fluidized bed, and non – uniform adsorbate distribution on the BAC, and displacement of lighter compounds with heavier ones in the fixed bed.

ACKNOWLEDGMENT

Firstly, I would like to express my sincere gratitude to Dr. Zaher Hashisho for his supervision, guidance, and support through my course work and research. His expertise and knowledge were essential for accomplishing this work.

I gratefully acknowledge the financial support from Ford Motor Company, Natural Science and Engineering Research Council (NSERC) of Canada, Alberta Advanced Education and Technology, and Canada Foundation for Innovation (CFI).

I would like to thank my colleagues especially Pooya Shariaty and Masoud Jahandar Lashaki in air quality and control research characterization laboratory for their assistance, availability and suggestions in my experiments.

I would like to appreciate Dr. John D. Atkinson for his revisions and recommendations to improve this document.

I also thank Dr. Haiyan Wang for her assistance in starting my GC – MS experiments.

I extend my appreciation to the technicians within the Civil and Environmental Engineering Department at the University of Alberta: Chen Liang and Elena Dlusskaya.

TABLE OF CONTENTS

CHAPTER 1: INTRODUCTION.....	1
1.1 Introduction	1
1.1.1 Volatile organic compounds	1
1.1.2 VOC abatement techniques.....	2
1.1.3 Adsorption process.....	4
1.2 Objectives	4
1.3 Thesis outline	5
CHAPTER 2: LITERATURE REVIEW	6
2.1 Adsorption	6
2.2 Adsorbent	6
2.3 Adsorption isotherms	9
2.4 Characterization of carbon materials.....	11
2.5 Functional groups on activated carbon.....	12
2.6 Factors controlling Adsorption.....	13
2.6.1 Adsorbent properties	14
2.6.2 Adsorbate properties	16
2.6.3 Adsorption conditions	18
2.7 Desorption	24
CHAPTER 3: MATERIALS AND METHODS	29
3.1 Materials	29
3.1.1 Adsorbent	29
3.1.2 Adsorbate	30
3.2 Methods	32
3.2.1 Adsorption and regeneration processes.....	32

3.2.2	Characterization tests	35
3.2.3	Thermo – gravimetric analysis.....	36
3.2.4	Gas chromatography – mass spectrometry analysis	37
3.2.5	Fluidization calculation.....	38
CHAPTER 4:	RESULTS AND DISCUSSION	41
4.1	Adsorption and desorption processes	41
4.1.1	Breakthrough profiles	41
4.1.2	Adsorption capacity	45
4.1.3	Regeneration efficiency	48
4.2	Characterization tests	52
4.2.1	Thermo – gravimetric analysis (TGA).....	52
4.2.2	Micropore – mesopore analysis	54
4.3	Homogeneity of the adsorption – desorption bed	56
4.4	Gas chromatography – mass spectrometry (GC – MS).....	58
CHAPTER 5:	CONCLUSION AND RECOMMENDATION	68
5.1	Conclusion.....	68
5.2	Recommendations	69
REFERENCES:	71
Appendix A:	Mass balance for adsorption of 500 ppmv 1,2,4 – trimethylbenzene on virgin BAC.....	81
Appendix B:	five cycles of Adsorption – desorption of 1,2,4 – trimethylbenzene on BAC	82
Appendix C:	Mass balance for adsorption of 500 ppmv VOC mixture on virgin BAC	85
Appendix D:	five cycles of Adsorption – desorption of VOCs’ on BAC	87

LIST OF TABLES

Table 1-1 VOC removal methods advantages and disadvantages (Khan and Ghoshal, 2000; Parmar and Rao, 2009)	3
Table 3-1 Elemental composition of virgin BAC by XPS	30
Table 3-2 Composition of the VOCs' mixture	31
Table 3-3 Indan physical and chemical properties.....	37
Table 3-4 Equations' parameters description and value	39
Table 4-1 Average energy consumption (in MJ) for all the experiments during 3-hour regeneration heating.....	51
Table 4-2 Characterization summary for 5 th cycle regenerated BAC samples loaded previously with VOC mixture	55

LIST OF FIGURES

Figure 2-1 Adsorption isotherm types due to IUPAC classification, adapted from (Bansal and Goyal, 2005).....	10
Figure 3-1 Pore size distribution of virgin beaded activated carbon (adapted from (Jahandar Lashaki et al., 2012b))	29
Figure 3-2 Schematic of the adsorption – desorption setup.....	33
Figure 3-3 TGA temperature program diagram.....	37
Figure 4-1 Breakthrough curves for five consecutive adsorption cycles of 1,2,4 – trimethylbenzene on BAC using different adsorption bed configurations (a) Fixed bed and (b) Fluidized bed	42
Figure 4-2 Breakthrough curves for five consecutive adsorption cycles of a VOC mixture on BAC using different adsorption bed configurations (a) Fixed bed and (b) Fluidized bed	44
Figure 4-3 Comparing the adsorption capacity of the virgin BAC for (a) 1,2,4 – trimethylbenzene and (b) VOCs’ mixture in different configurations accompanied by the standard deviation error bars	46
Figure 4-4 Comparing the cumulative heel formation after five cycles adsorption-desorption of (a) 1,2,4 – trimethylbenzene and (b) VOC mixture on BAC in fixed bed and fluidized bed adsorption configurations accompanied by standard deviation error bars	49
Figure 4-5 Temperature profile during fixed bed desorption of (a) 1,2,4 – trimethylbenzene (b) VOC mixture from BAC. The adsorbents were loaded by fixed bed and fluidized bed adsorption configuration.	50
Figure 4-6 TGA results for the 5 th cycle regenerated BAC samples loaded previously with (a) 1,2,4 – trimethylbenzene and (b) VOC mixture	53
Figure 4-7 Effect of adsorbent bed configuration on pore size distribution of the regenerated BACs previously loaded with VOCs’ mixture after five cycles	55
Figure 4-8 TGA results for regenerated BAC after one cycle adsorption from top, middle, and bottom of the reactors (a) 1,2,4 – trimethylbenzene and (b) VOC mixture	57

Figure 4-9 Effluent concentration during adsorption of modified VOC mixture on BAC in order of the components' retention time in GC (The boiling points are shown by the components in the legends) using (a) fixed bed and (b) fluidized bed configuration. The second axis on the right demonstrates the total adsorbates concentration measured by GC – MS and FID in the effluent..... 61

Figure 4-10 Effluent concentration of (a) n – butanol and (b) n – butyl acetate during adsorption on BAC using GC-MS..... 63

Figure 4-11 Concentrations of the organic species in the desorbing gas during regeneration of BAC previously saturated with modified VOC mixture using (a) fixed bed configuration and (b) fluidized bed configuration 66

LIST OF ABBREVIATIONS AND NOMENCLATURE

ACF	Activated Carbon Fiber
ACFC	Activated Carbon Fiber Cloth
BAC	Beaded Activated Carbon
BET	Brunauer, Emmett, and Teller Theory
BP	Boiling Point
COP	Critical Oxidation Potential
DAC	Data Acquisition and Control
DFT	Density Functional Theory
DNA	Deoxyribonucleic Acid
EPA	Environmental Protection Agency
FID	Flame Ionization Detector
GAC	Granular Activated Carbon
GC – MS	Gas Chromatography – Mass Spectrometry
HAP	Hazardous Air Pollutant
IAST	Ideal Adsorbed Solution Theory
IUPAC	International Union of Pure and Applied Chemistry
MEK	Methyl Ethyl Ketone
MP	Micropore Method
MTZ	Mass Transfer Zone
MW	Molecular Weight
NO _x	Nitrogen Oxides
PAC	Powdered Activated Carbon
PAN	Peroxy Acetyl Nitrate
PID	Photo – Ionization Detector
PPMV	Parts Per Million (Volume fractions)
PSR	Pressure Swing Regeneration
pH _{PZC}	pH of Point of Zero Charge
SAC	Spherical Activated Carbon
SCCM	Standard Cubic Centimeters per Minute

SLPM	Standard Liter per Minute
TGA	Thermo – Gravimetric Analysis
TPD	Temperature Programmed Desorption
TSR	Temperature Swing Regeneration
VOC	Volatile Organic Compounds
WAO	Wet Air Oxidation
XPS	X – ray Photoelectron Spectroscopy

CHAPTER 1: INTRODUCTION

1.1 Introduction

1.1.1 Volatile organic compounds

Volatile organic compounds (VOCs) emissions in gaseous and aqueous streams should be controlled because of their health and environmental impacts. Many VOCs are toxic and can cause headaches, eye, nose and throat irritations, nausea, dizziness, memory loss, and damages to the liver, central nervous system, and lungs (Environmental Protection Agency; Kampa and Castanas, 2008; Leslie, 2000). Some VOCs are carcinogenic and mutagenic for human and animals even when inhaled at concentrations as low as 0.25 ppm (Pariselli et al., 2009). Some VOCs deplete the stratospheric ozone layer (Atkinson, 2000; Lillo-Ródenas et al., 2005), or are precursors for formation of tropospheric ozone (ground – level ozone) (Bowman and Seinfeld, 1995).

According to the 1990 amendment to the US Clean Air Act, about 97 of 189 hazardous air pollutants (HAPs) are VOCs. For this reason, strict regulations were set for VOC emissions in 1990 (Parmar and Rao, 2009). In the USA, VOC emissions in 2012 from industrial processes, transportation, and fuel combustion was 1.1×10^{10} kg (Environmental Protection Agency, 2013).

VOCs can be released from organic solvents, glues, adhesives, agricultural operations, gasoline leakage during loading, fuel combustion, petroleum refineries (Environmental Protection Agency; Ramalingam et al., 2012; Tancrede et al., 1987) and painting processes including automotive painting booths (Kim et al., 1997). About 6.58 kg of VOCs are used as paint solvents per vehicle in a typical automotive painting operation in North America (Kim, 2011).

Concerns about VOC health and environmental impacts triggered an interest in developing novel treatment techniques for controlling their emissions.

1.1.2 VOC abatement techniques

There are many treatment techniques for controlling or destroying VOCs emissions before they are released (Khan and Ghoshal, 2000). Selecting the most effective treatment technique depends on many parameters including pollutant type, source, concentration, flow rate, presence of compounds other than VOCs, reusability of captured compounds, regulatory limits, safety, location, cost, and operative possibility of the selected technique (Cooper and Alley, 2002; Lillo-Ródenas et al., 2005; Parmar and Rao, 2009).

Treatment techniques used for indoor and outdoor air quality control are categorized as destructive or recovery methods. Destructive methods are used when recovering the removed compounds is not necessary or economical. For these methods, the VOCs are converted to other, non-hazardous chemical compounds, often CO₂ and H₂O. The most well-known destruction methods are bio-filtration and oxidative treatment techniques including photocatalysis, thermal oxidation, and catalytic oxidation (Berenjian et al., 2012).

For recovery methods, organic compounds are removed in a way that they can be recovered for reuse. Common recovery techniques include absorption, adsorption, condensation, and membrane separation for gaseous and liquid streams (Khan and Ghoshal, 2000; Parmar and Rao, 2009).

Table 1-1 summarizes advantages and disadvantages associated with each gas treatment technique. The demerit of secondary generation of waste can be associated with most methods, including biomass formation in biological processes, production of greenhouse gases in oxidative methods, condensate in condensation, and spent adsorbent in adsorption (Parmar and Rao, 2009).

Table 1-1 VOC removal methods advantages and disadvantages (Khan and Ghoshal, 2000; Parmar and Rao, 2009)

Removal method	Advantages	Disadvantages
Adsorption on activated carbon	<ul style="list-style-type: none"> • Appropriate for low concentration VOCs (Sullivan et al., 2004), • Does not have problem with high inlet concentrations and fluctuations (Hashisho et al., 2008; Sullivan et al., 2004), • Allow energy recovery by using fuel reformer or fuel cell (Wherrett and Ryan, 2004), • Allow VOC recovery, • Not much limitation on VOCs properties (boiling point, biodegradability) 	<ul style="list-style-type: none"> • Sensitive to humidity, • Risk of fire
Bio-filtration Biological removal	<ul style="list-style-type: none"> • Appropriate for low concentration VOCs, • allow energy recovery by paint sludge (Kim, 2011) 	<ul style="list-style-type: none"> • Low removal efficiency, and Slow process, • Cannot tolerate high and fluctuating concentrations of pollutants (Hashisho et al., 2008; Sullivan et al., 2004), • Limitation on type of pollutant to be biodegradable, • Recovery of VOCs are not possible
Condensation	<ul style="list-style-type: none"> • Good recovery of the VOCs possible 	<ul style="list-style-type: none"> • Low removal efficiency, • Not cost effective for low VOC concentrations (Mohan et al., 2009), • Applicable for low boiling point compounds (<30°C)
Catalytic methods	<ul style="list-style-type: none"> • Moderate energy recovery 	<ul style="list-style-type: none"> • Pollutants has to be non-poisonous to the catalyst
Thermal oxidation Oxidative methods	<ul style="list-style-type: none"> • High energy recovery (Kim, 2011; Wherrett and Ryan, 2004) 	<ul style="list-style-type: none"> • Not cost effective for low VOC concentrations, • Needs combustion products treatment process

The main references were cited in the table heading, confirming some information with other papers within the table.

According to the mentioned merits and demerits, adsorption has emerged as one of the energy efficient and cost effective techniques used for removing low concentration ($< 10,000$ ppm) VOCs from gaseous streams (Bansal and Goyal, 2005; Fletcher et al., 2006; Popescu et al., 2003). For this reason adsorption on activated carbon was chosen as the VOC removal method in this research, where VOC concentrations of 500 ppmv are investigated.

1.1.3 Adsorption process

Adsorption, using activated carbon, zeolite, or molecular sieve adsorbents, regularly removes more than 80% of VOCs from gas and liquid streams (Bansal and Goyal, 2005). Adsorption, when cycled with desorption methods, allows for VOC recovery and adsorbent regeneration (Busca et al., 2008; Parmar and Rao, 2009). Desorption process is also a challenge associated with adsorption treatment method which determines the recovery of the VOCs after removal and adsorbent regeneration efficiency. Irreversible adsorption is the incomplete desorption of adsorbates during adsorbent regeneration. Previous studies have investigated parameters influencing irreversibility of adsorption for different adsorbates and adsorbents and tried to eliminate this irreversibility by modifying the adsorption and desorption procedures used for this purpose (Aktaş and Çeçen, 2006; Hashisho et al., 2005; Jahandar Lashaki et al., 2012b; Sullivan et al., 2001; Wang et al., 2012).

1.2 Objectives

The goal of this research is to determine the effect of adsorption bed configuration on the irreversible adsorption of volatile organic compounds from the gas-phase. 1,2,4 – trimethylbenzene and a mixture of nine VOCs were used as adsorbates and beaded activated carbon (BAC) was used as the adsorbent. The main objectives of this research are:

1. To investigate the effect of adsorption bed fluidization on the adsorption capacity and irreversible adsorption of a single organic compound and a mixture of VOCs on BAC

2. To study the effect of adsorption bed configuration on competitive adsorption of VOCs on BAC.

Many industries use activated carbon adsorption to reduce their VOC emissions to the atmosphere. The adsorption process has the advantage of adsorbate recovery and adsorbent regeneration for reuse; and many investigations have been completed to improve the performance of adsorption and desorption processes. However, there is a knowledge gap about the configuration of the adsorbent bed and how it influences irreversible adsorption during desorption. This is important to understand because large scale industrial processes often use fluidized bed systems to minimize pressure drop, but irreversible adsorption research has focused exclusively on fixed bed systems.

1.3 Thesis outline

This thesis consists of five chapters which will contribute to fulfill the overall objective of this research. Chapter 1 provides an introduction about the background and goal of the research. A general literature review about adsorption, including descriptions of different adsorbents, adsorbates, process conditions, and regeneration processes, is included in Chapter 2. Chapter 3 explains the materials and methods used for completion of this research. Experimental results and corresponding discussions are presented in Chapter 4, and major conclusions derived from this work as well as recommendations for future work are presented in Chapter 5.

CHAPTER 2: LITERATURE REVIEW

2.1 Adsorption

In this chapter, a literature review describing adsorption as a common technique for capturing organic compounds from gaseous and aqueous streams was prepared. Adsorption is the process of attaching a molecule (adsorbate) to surface of a solid or liquid (adsorbent). For solid adsorbents, weak or strong interactions are formed, for example, via electrostatic forces, dispersive forces, or covalent bonding (Suzuki, 1990). Adsorption can be categorized as physisorption and chemisorption (Bansal and Goyal, 2005). Physisorption, which corresponds to weak interaction forces (often van der Waals forces) between the adsorbent and adsorbate, is reversible. Van der Waals forces can be caused by London dispersion forces or classical electrostatic forces (Singh et al., 2002). Chemisorption, which is generally irreversible, corresponds to strong interaction forces between the adsorbate and adsorbent and is often associated with the formation of covalent bonds (Yang, 1997).

Adsorption is exothermic as it is accompanied by the release of heat. Adsorption enthalpy is slightly higher than adsorbate vaporization enthalpy in physisorption and is similar to the reaction energy spent on chemical bond formation during chemisorption. Adsorption enthalpy depends on both adsorbate and adsorbent, as well as adsorption conditions including temperature and pressure (Bottani and Tascón, 2008; Cooper and Alley, 2002).

2.2 Adsorbent

Porous materials with varying physical (e.g., adsorbent structure and pore size distribution) and chemical (e.g., surface functional groups and polarity) properties can be effective as VOC adsorbents depending on the adsorption conditions and adsorbate properties. Porous materials are effective adsorbents because of their high internal surface area and extensive porous structure (Parmar and Rao, 2009). The International Union of Pure and Applied Chemistry (IUPAC)

identify adsorbents' pores depending on their diameters; micropores (less than 2 nm), mesopores (between 2 to 50 nm), and macropores (more than 50 nm) (Bansal and Goyal, 2005). Gas phase adsorption primarily occurs in micropores and mesopores. Micropores decrease diffusion pathways, thus increasing adsorption capacity and improving adsorption kinetics. Surface functional groups on adsorbents can also influence their adsorptive behavior (Yang, 1997). Adsorbents used for VOC control include carbonaceous and non-carbonaceous materials, though carbon – based materials are regularly found to be efficient and economical for VOC capture (Bottani and Tascón, 2008).

2.2.1.1 Non – carbon based adsorbents

Most non – carbonaceous adsorbents used for VOC adsorption are zeolite – based. Hydrophobic zeolites have the advantages of thermal stability, hydrophobicity, precise pore size distributions, selective adsorption, and non – flammability (Khan and Ghoshal, 2000; Parmar and Rao, 2009; Su et al., 2009).

Activated alumina, silica gel (Suzuki, 1990), modified mesoporous silica (Silvestre-Albero et al., 2010), silica alumina and impregnated silica alumina (Bouhamra et al., 2009), polymeric adsorbents, and other porous inorganic materials (Busca et al., 2008) are among the non – carbon based materials documented for VOC adsorption. Novel adsorbents also continue to be introduced for VOC adsorption, including mesoporous chromium oxide, silica fiber matrix (Parmar and Rao, 2009) and monolithic adsorbents (Lapkin et al., 2004). To date, these materials are not industrially relevant because of the high costs associated with adsorbent production.

2.2.1.2 Carbon – based adsorbents

Carbon – based materials have long been considered cost effective and efficient for air cleaning applications (Bansal and Goyal, 2005; Bottani and Tascón, 2008) and their first documented use was in 1600 B.C. in Egypt for medical purposes (Suzuki, 1990). A major advantage for these materials is that they can be tailored to have different physical and chemical characteristics

(Silvestre-Albero et al., 2010). Activated carbon showed high adsorption capacity for removing low concentrations of organic compounds from gaseous and aqueous streams (Carratalá-Abril et al., 2009; Dąbrowski et al., 2005; Pires et al., 2003) and for removing micro – pollutants with low molecular weight and metals in water and wastewater treatment processes (Álvarez et al., 2004; Lu and Sorial, 2009). For many VOC adsorption applications, the high adsorption capacity of activated carbon can be attributed to its high specific surface area (Huang et al., 2003), high volume of micropores (Kim et al., 2001; Lillo-Ródenas et al., 2005), and low concentration of surface oxygen groups (Carratalá-Abril et al., 2009). Negatives of activated carbon adsorbents include flammability, regeneration difficulties when adsorbing high boiling point compounds, competitive adsorption in high relative humidity streams, and potential to oxidize or decompose select adsorbates into other toxic compounds (Khan and Ghoshal, 2000; Parmar and Rao, 2009).

There are many types of activated carbon available with different pore size distributions, surface characteristics, and shapes (e.g., pelletized, granular, powdered, and spherical). The porous structure and surface functional groups of activated carbons depend on their precursor materials, activation method and conditions (e.g., temperature and oxygen), and post – treatment reactions (Boulinguez and Le Cloirec, 2010; Chiang et al., 2001b; Dąbrowski et al., 2005).

Coal, wood, nutshells, bamboo, coconut shell, lignite, sawdust, petroleum coke, peat, synthetic polymers, biomass materials, and agricultural by – products are among the many raw materials used as activated carbon precursors (Chiang et al., 2001a; Huang et al., 2002; Rivera-Utrilla et al., 2003; Tsai et al., 2008). These materials have low inorganic content, are generally inexpensive and readily available, and are stable during storage (Dąbrowski et al., 2005).

Carbon activation (i.e., the addition of pores to a primarily carbonaceous solid) can be completed by physical or chemical procedures. In physical activation, the raw materials are first carbonized in an inert atmosphere (600 – 900°C) and then are partially gasified in steam or CO₂ (600 – 1000°C). High

gasification resulting from increased temperature or a more oxidizing atmosphere results in higher burn – off of carbon. Carbonization and gasification time, temperature, and reactive gas influence the activated carbon's pore size. Higher burn – off results in more microporosity for CO₂ activation, while steam leads to wider micropore distributions and increased mesoporosity (Ahmad and Idris, 2013). Chemical activation includes simultaneous carbonization of the raw material and activation, and is performed at lower temperatures (400 – 900°C). The carbon precursor is first impregnated with activating agents including KOH, ZnCl₂, H₃PO₄, ammonia, or H₂O₂ and then heated in an inert atmosphere (Ahmad and Idris, 2013; Huang et al., 2002; Wang and Kaskel, 2012). Temperature, chemical agent, and impregnation ratio affect the properties of the activated material. Compared to physical activation, chemical activation is easier to develop a desired pore size distribution (Ahmadpour and Do, 1996).

2.3 Adsorption isotherms

Adsorption isotherms describe the capacity of an adsorbent for a specific adsorbate at varying concentrations or relative pressures and at a constant temperature (Cooper and Alley, 2002). Adsorption isotherms have five main types according to IUPAC categorization, as shown in Figure 2-1. Horizontal and vertical axes represent the adsorbate's concentration in the liquid/gas phase and on the adsorbent, respectively. Type I, IV, and V adsorption isotherms are common for porous materials. The porous structure of adsorbents can be better understood from their adsorption isotherms. Mesoporous adsorbents show an ascending slope at high concentrations while microporous materials plateau at high concentrations (Carratalá-Abril et al., 2009). Type I isotherms are representative of microporous adsorbents for which monolayer coverage occurs at low adsorbate concentrations. Type II and Type III isotherms describe complete multilayer accumulation of adsorbates on non – porous or highly macroporous materials with weaker adsorbate – adsorbent interactions in Type III. Type IV isotherms are indicative of a mesoporous/microporous material that switches from monolayer adsorption to multilayer due to capillary condensation in the pores and

Type V demonstrates porous adsorbent with weak adsorbate – adsorbent interactions similar to Type III (Bansal and Goyal, 2005; Bottani and Tascón, 2008; McEnaney, 1988).

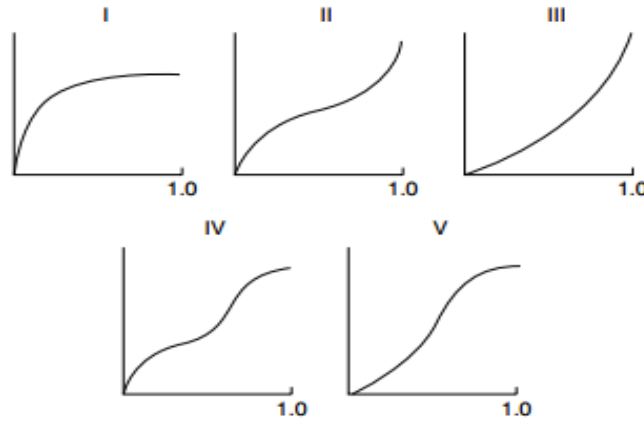


Figure 2-1 Adsorption isotherm types due to IUPAC classification, adapted from (Bansal and Goyal, 2005)

Quantitative models have been developed for different adsorbate – adsorbent systems to simplify understanding the adsorption process at different conditions. The Langmuir isotherm (Equation 2-1) is a simple model used for both physical and chemical adsorption of gases (Bansal and Goyal, 2005; Benkhedda et al., 2000; Langmuir, 1918; Pei and Zhang, 2012; Yang, 1997).

$$C_s = \frac{q_m b C_g}{1 + b C_g} \quad 2-1$$

C_s (mg/g) and C_g (mg/m³) are the equilibrium adsorbate concentration in solid and gas phase, respectively. q_m (mg/g) is the maximum adsorption capacity and b (m³/mg) is the affinity constant which represents the strength of adsorbate – adsorbent interactions. The Langmuir isotherm is appropriate for monolayer adsorption, which can occur in select physisorption scenarios (e.g., low adsorbate concentrations, narrow micropores) or during chemisorption.

The Freundlich empirical isotherm model (Equation 2-2) is also used for modeling VOC adsorption on activated carbon (Bansal and Goyal, 2005; Chuang et al., 2003b).

$$C_s = KC_g^{1/n} \quad 2-2$$

Where, C_s (mg/g) and C_g (mg/m³) have the same definitions as in the Langmuir equation. K and n are model constants dependent on temperature and adsorbate – adsorbent interactions (Benkhedda et al., 2000). Unlike the Langmuir model, the Freundlich isotherm accounts for multiple adsorption layers.

Boulinguez and Le Cloirec (2010) used a combination of Langmuir and Freundlich equations to model the adsorption behavior of five VOCs on four different types of activated carbons.

The semi-empirical Dubinin – Radushkevich (DR) equation, based on the Polanyi theory (Yang, 1997) and micropore filling theory, also is used to investigate adsorption on activated carbons (Bansal and Goyal, 2005; O'Connor and Mueller, 2001). The model considers the adsorbate's affinity to the adsorbent (Benkhedda et al., 2000) as well as the adsorbate's kinetic diameter (Jahandar Lashaki et al., 2012a) to better predict adsorption capacity. Hung and Lin (2007) concluded that the Langmuir model should be used for low concentrations adsorbates, while the DR model better fits high concentration species.

Furthermore, there are isotherm models more recently being developed to describe adsorption of binary and multicomponent adsorbates. The ideal adsorbed solution theory (IAST) by Myers and Prausnitz suggested isotherm models for mixtures' adsorption (Yang, 1997).

2.4 Characterization of carbon materials

To better understand adsorption performance and to isolate the efficacy of activation and regeneration, it is necessary to characterize the physical and chemical properties of the material. Pore size measurements were first done by Kelvin using a cylindrical model to represent pores and based on capillary

condensation for relative pressures higher than 0.42 (Bottani and Tascón, 2008; Chiang et al., 2001a). Lippens and de Boer (1965) developed a method for measuring pores at lower relative pressures that was later modified by Mikhail et al. (1968) as the micropore (MP) method. The Brunauer, Emmett and Teller (BET) method allows for the determination of specific surface area at relative pressures lower than 0.14 (Chiang et al., 2001a). This method is based on adsorption of a gas at low temperatures to form physical forces with adsorbent surface assuming monolayer adsorption developed by Langmuir isotherm for all the adsorbed layers, similar adsorption energy on homogenous adsorbent sites, and no intermolecular interactions between the layers (Ahmad and Idris, 2013; Brunauer et al., 1938). The BET isotherm is obtained by N₂ (gas diameter of 0.36 nm) at 77 K or CO₂ (gas diameter of 0.33 nm) at 273 K. Carbon dioxide adsorption is used to determine dimensions of narrow micropores because it has lower diffusion resistance than nitrogen (Cazorla-Amorós et al., 1996; Lillo-Ródenas et al., 2005). Argon (gas diameter of 0.34 nm) can also be used for detecting narrow micropores in activated carbon (Chiang et al., 2001a; Dombrowski et al., 2000; Yang et al., 2012).

Density functional theory (DFT) is used to determine the micro and mesopore size distribution by using the nitrogen adsorption isotherm. In this theory, the pores are assumed to be semi-infinite and slit shaped with homogenous energetic site distribution on thick walls, while surface heterogeneity causes no significant deviations in the model results (Dombrowski et al., 2000; Olivier, 1998; Ravikovitch and Neimark, 2006).

2.5 Functional groups on activated carbon

Generally, about 90% of the activated carbon structure consists of stable basal planes that have low potential for chemical reactions than edges (Bansal and Goyal, 2005; Franz et al., 2000). The remaining structure consists of different functional groups and inorganic ash (Villacañas et al., 2006). Potential oxygen functional groups on activated carbon are carboxyl, phenol, lactone, aldehyde, ketone, quinone, hydroquinone, and anhydride (Bansal and Goyal, 2005). Surface

nitrogen and sulfur groups might also be present depending on the activated carbon precursor.

Acidic and basic functional groups can be generated on carbon during activation or during post – production electrochemical or heat treatments. Exposure to air after activation may lead to formation of oxygenated groups on activated carbon surface (Dąbrowski et al., 2005). On the other hand, thermal activation in inert atmosphere mostly eliminates acidity (surface oxygen functional groups) of the activated carbon (Aktaş and Çeçen, 2006; Lillo-Ródenas et al., 2005).

Methods available for quantifying functional groups on carbon include acid – base titrations (e.g., Boehm Titrations) (Villacañas et al., 2006), Fourier transform infrared spectroscopy (FTIR), x – ray photoelectron spectroscopy (XPS) (Kaneko et al., 1995), temperature programmed desorption (TPD) (Popescu et al., 2003), and pH_{pzc} (pH of the point of zero charge) measurement (Dąbrowski et al., 2005).

2.6 Factors controlling Adsorption

Adsorption capacity and kinetics are influenced by many factors. Recognizing these factors and understanding their significance helps to better predict adsorption. Many studies strive to optimize their process parameters and adsorbent properties to more efficiently control VOC emissions.

Adsorption isotherms, mass transfer zone (MTZ), and adsorbate breakthrough profiles can demonstrate the effectiveness of a particular adsorbent. Changes to results presented by these methods can also be used to quantify the impacts of changing process parameters on an adsorbent – adsorbate system.

Adsorption isotherms depict the adsorption capacity for a selected adsorbent at increasing adsorbate concentrations and also gives information about the adsorbent structure (Bansal and Goyal, 2005; Fletcher et al., 2006).

Breakthrough curves show the amount of non – adsorbed adsorbate that passes through an adsorbent bed. Breakthrough time is generally defined as the time when adsorbate emission starts and adsorbent bed saturation (saturation time) occurs when the adsorbents are not adsorbing anymore (Carratalá-Abril et al., 2009). Adsorption capacity is calculated by determining the area under the breakthrough curve (integration). The shape of the breakthrough curve and, in particular, the slope incurred between breakthrough time and saturation time, describe the system's MTZ. When the MTZ reaches the end of the adsorbent bed, breakthrough begins and when it leaves, the adsorbents are saturated. A longer MTZ, visualized as a lower slope on the breakthrough curve, depicts slower adsorption kinetics (Mohan et al., 2009).

Factors influencing adsorption process are the adsorbent's physical and chemical characteristics, adsorbate properties, and adsorption conditions (Huang et al., 2003). These parameters effects were explained in sections 2.6.1 to 2.6.3.

2.6.1 Adsorbent properties

An adsorbent's pore size distribution, specific surface area, and pore volume influence its ability to adsorb a particular adsorbate (Chakma and Meisen, 1989).

Higher surface area of the activated carbon prepares more sites for the VOCs to be adsorbed which results in higher adsorption capacities in the case that the pore size is appropriate for the selected VOCs (Chiang et al., 2001b; Tsai et al., 2008). Tsai et al. (2008) obtained high capacity for adsorption of VOCs (acetone, chloroform, acetonitrile) from gaseous stream using ACF with high micropore specific surface area.

The effect of adsorbent total pore volume and specific surface area has to be studied in detail of its pore size distribution and adsorbate physical properties as molecular size (Chakma and Meisen, 1989; Huang et al., 2002). Huang et al. (2002) discussed the effect of pore size distribution on adsorption of acetone and n – hexane and attributed the difference in adsorption characteristics to diffusion

of the different sized adsorbates into the adsorbent. Carratalá-Abril et al. (2009) emphasized the importance of narrow micropores (less than 0.7 nm) for obtaining longer breakthrough and saturation times when adsorbing low concentration toluene with activated carbon, but also mentioned that narrow micropores can influence the breakthrough curve slope for different adsorbates with various sizes. Lillo-Ródenas et al. (2005, 2011) similarly presented high adsorption capacities for low concentrations of toluene and benzene on different activated carbon fibers (ACF) with narrow micropores compared to granular activated carbon (GAC) and powdered activated carbon (PAC) with lower narrow micropores volume. Higher VOC adsorption capacity has been described for activated carbon fiber cloth (ACFC) compared to GAC because of the higher fraction of narrow micropores available in ACFC (Boulinguez and Le Cloirec, 2010; Das et al., 2004; Sullivan et al., 2004). On the other hand, Lin et al. (2013) concluded that mesopores are relevant when adsorbing high concentrations of VOCs (toluene) since the amount of adsorbed was more than the filled micropores volume.

Besides GAC, PAC, ACF, and ACFC, spherical activated carbon (SAC) and beaded activated carbon (BAC) are also used as microporous adsorbents, for VOC removal, with high microporosity, low oxygen content, and high purity which showed appropriate adsorption capacity for VOCs (Jahandar Lashaki et al., 2012a; Jahandar Lashaki et al., 2012b; Romero-Anaya et al., 2010; Wang et al., 2012; Wang et al., 2009). BAC was also used in this research as VOC removal adsorbent.

Aktaş and Çeçen (2006) and Huang et al. (2002) presented surface accessibility, diffusion path, and chemical properties of the adsorbent as more important factors than total surface area for determining adsorption capacity. Others, however, have found adsorbent physical properties to be notably more relevant for determining capacity (Díaz et al., 2005; Tsai et al., 2008). When selecting an adsorbent, therefore, it is important to consider both the adsorbent's physical and chemical properties.

High oxygen content (e.g. carboxylic groups) on activated carbon's surface may result in high adsorption of water, which is undesirable for VOC control. Moreover, for more hydrophilic activated carbons, higher adsorption of some molecules such as hydrides can occur (Sullivan et al., 2007). Fletcher et al. (2007) had similar conclusions for adsorbents with similar pore size distribution but different functionalities.

(Li et al., 2011) experimented with different chemical agents in activation of coconut shell based carbon for adsorption of hydrophobic VOC (O – xylene), obtaining higher adsorption capacity in case of alkali (ammonia, sodium hydroxide) treated GAC in comparison to the adsorbents modified with acids. The authors concluded that lower surface oxygen groups (surface acidity) are more favorable for hydrophobic VOC adsorption.

2.6.2 Adsorbate properties

Adsorbate physical and chemical properties also influence their adsorption onto activated carbon, as highlighted in many research articles. Molecular weight, size, structure, functional groups, polarity, and boiling point are among the most discussed parameters.

Li et al. (2012) studied the role of adsorbate molecular weight, size, boiling point, and density when adsorbing xylene, toluene, and acetone on activated carbon. The authors found a linearly increasing relationship between adsorption capacity and mentioned adsorbate properties in the condition of availability of higher pore size than the molecular dynamic diameter.

Jahandar Lashaki et al. (2012b) and Wang et al. (2012) also investigated the adsorption of organic compounds with varying molecular weights, molecular sizes, and boiling points on activated carbon. Jahandar Lashaki et al. (2012b) concluded that the accumulation of high molecular weight molecules with bulky structures in carbon micropores can cause pore blockage, preventing the subsequent adsorption of smaller molecules. Pore blockage can also happen when

low molecular weight compounds are displaced by larger, high boiling point ones (competitive adsorption) (Kim et al., 2001; Wang et al., 2012).

The molecular size of the adsorbate affects the adsorption rate because diffusion can be a limiting factor (Salvador and Jiménez, 1996). For an adsorbent with very narrow pores, larger diameter adsorbates will diffuse more slowly, or possibly be unable to enter the pores of the adsorbent. Molecular size and dynamic diameter are important factors used in the D – R isotherm model for predicting adsorption (Hung and Lin, 2007; Jahandar Lashaki et al., 2012a).

Hydrophobic and hydrophilic sites on activated carbon produced during activation or post – production chemical treatments alter the polarity of the adsorbent, making the polarity of the adsorbate an important parameter to consider. (Fletcher et al., 2006) and Lee et al. (2006) concluded adsorbate dipole moment affects adsorption by comparing acetone (polar) and toluene (non – polar) adsorption on a hydrophobic adsorbent, finding that polar compounds showed increased affinity for hydrophilic adsorbent sites. Chiang et al. (2001b) also found higher adsorption capacity of non – polar adsorbates on carbons with less oxygen content by comparing adsorption of VOCs with different dipole moments on adsorbents with different physical and chemical properties. They concluded that surface area and pore volume (regardless of the pore size) are more influential on adsorption capacity than polarity of the adsorbate and functionality of the adsorbent.

Kawasaki et al. (2004) investigated the effect of boiling point and molecular weight on adsorption of toluene, benzene, and xylene and by studying adsorption of o-, m-, and p-xylene, the authors could focus on the relevance of chemical structure, removing molecular weight and boiling point variables. They found the adsorption capacity to be relevant to the difference of melting and boiling point of the adsorbates and not only the boiling point and also concluded structure to be effective on adsorption kinetics.

Adsorbate boiling point is important in gas – phase adsorption since higher boiling point adsorbates, are more adsorbed by activated carbon because of capillary condensation more readily occurs (Li et al., 2012). O'Connor and Mueller (2001) demonstrated the effect of heat of vaporization or boiling point in adsorption and breakthrough of VOCs on GAC using D – R equation and predicted breakthrough using the heat of vaporization of the adsorbates during adsorption and competitive adsorption.

Some researchers have shown that adsorbate boiling point can be more influential than polarity for adsorption of high boiling point compounds as Biron and Evans (1998) stated, compounds with higher boiling point than water can replace the water molecules already adsorbed on activated carbon.

Moreover some adsorbents with specific pore size distributions can only adsorb molecules with specific kinetic diameters from the mixture, which can be used for separation purposes (Lu and Sorial, 2004, 2009).

In conclusion, it is important to consider all aspects of adsorbate and adsorbent properties to predict an adsorption capacity and kinetics. Researchers found that in most cases, surface area and pore size characteristics of the adsorbent, and adsorbate properties including molecular weight, structure, and boiling point are the most important parameters for capturing VOCs from gaseous streams.

2.6.3 Adsorption conditions

2.6.3.1 Temperature

Since adsorption is exothermic, higher temperatures are expected to decrease adsorption capacity (Huang et al., 2003). Fire hazard is one of the crucial issues with high temperature adsorption of high concentration VOC streams (tested 20,700 ppm of acetone) especially ketones on activated carbon (Delage et al., 1999). While increased temperatures decrease adsorption capacity, they also cause more rapid adsorption kinetics by decreasing diffusion limitations (Chuang

et al., 2003a; Jahandar Lashaki et al., 2012b). Therefore, breakthrough time decreases with increasing temperature but the mass transfer zone is shorter (Chuang et al., 2003b).

It is important to note that increased adsorption temperature can inversely affect the physisorption while it can increase interactions between adsorbate and adsorbent (Chiang et al., 2001a), possibly causing irreversible chemisorption to occur (Jahandar Lashaki et al., 2012b).

Since heat is released during adsorption, adsorbent bed temperature increases can occur when carbon adsorbs high concentration VOC streams. Larger temperature increases are associated with gas phase adsorption than liquid phase adsorption because liquids have larger heat capacities (Delage et al., 1999; Yazbek et al., 2006). Kawasaki et al. (2004) also reported lower influence of temperature on adsorption of liquid stable compounds by comparing benzene and toluene adsorption at 288 and 298 K resulting in decreased the benzene saturation and no change in toluene adsorption.

2.6.3.2 Inlet concentration

Increasing adsorbate concentration increases adsorption capacity by increasing the concentration gradient. Among porous materials, the adsorption capacity of the mesoporous materials can be increased by increasing the inlet concentration by forming intra – layer and intermolecular interactions (Mohan et al., 2009). Pei and Zhang (2012) showed higher toluene capacity on activated carbon by increasing adsorbate concentration, although they described surface diffusion as the dominant mechanism. However, slower diffusion of adsorbates into the pores was reported due to higher surface coverage in case of high concentrations (Fletcher et al., 2006). Gas flow rates of pollutant streams also have effects on adsorption capacity and kinetics. Kawasaki et al. (2004) found higher flow rate increasing the adsorption capacity and kinetics in case of benzene. In contrast, Mohan et al. (2009) reported higher adsorbate diffusion and

adsorption capacity at lower flow rates because of increased contact time between adsorbate and adsorbent.

2.6.3.3 Relative humidity

Relative humidity hinders adsorption of VOCs because of competitive adsorption. Water molecules can be adsorbed on activated carbon by physisorption and pore – filling (in high concentrations) or chemical interactions (e.g., hydrogen bonding) with surface functional groups (at low concentrations on hydrophilic adsorbents or activated carbon with oxygen functional groups) (Franz et al., 2000; Kaneko et al., 1995; Sullivan et al., 2007). Water molecules attached to the surface of adsorbent can form clusters, clogging the entrances to micropores (Mahajan et al., 1980) and decreasing adsorption capacity (Huang et al., 2003). Competitive adsorption of water can be, at least partially, overcome when adsorbing compounds that have higher adsorption energy than water, allowing the desired adsorbate to displace unwanted water molecules (Biron and Evans, 1998; Delage et al., 1999; Sullivan et al., 2001).

One of the practical solutions to eliminate the effect of humidity is using hydrophobic adsorbents. Carbon based materials with no oxygen surface groups or some synthesized non – carbon based materials are hydrophobic and appropriate for low concentration VOC adsorption from humid gaseous streams (Parmar and Rao, 2009). In addition, a low amount of humidity may decrease temperature gains associated with VOC adsorption because of water vaporization which decreases the fire risks with activated carbon adsorption (Delage et al., 1999).

2.6.3.4 Oxic and anoxic conditions

The adsorbate's carrier gas being oxic or anoxic can also affect adsorption behavior. Many studied the effects in liquid phase adsorption but few focused on gaseous phase. Jahandar Lashaki et al. (2013) used air and nitrogen to provide oxic and anoxic atmospheres for VOC adsorption on activated carbon in the gas

phase, finding no difference in adsorption capacity for the virgin adsorbent but it affected the recovered adsorption capacities.

2.6.3.5 Adsorption Bed Configuration

It is important to consider the configuration of the adsorption bed because it can influence adsorption capacity, kinetics, irreversibility, and so desorption efficiency. Three common adsorption bed configurations used in experimental and industrial processes are fixed, moving, and fluidized bed. Adsorption kinetics, VOC removal efficiency, and regeneration conditions and efficiency are different for each configuration.

In fixed bed, gas is not distributed uniformly throughout the bed and clogging or gas channeling may occur. VOCs are adsorbed in zones with more contact between the adsorbate and adsorbent and the heat of adsorption may cause hot spots in these zones, possibly causing bed fires (Delage et al., 2000; Sanders, 2003; Yazbek et al., 2006). Fixed bed systems are also associated with high pressure drops, which can increase operational costs.

Advantages of using a fluidized bed adsorption configuration compared to a fixed bed configuration are improved faster adsorption kinetics, sharper breakthrough curves, continuous processing of adsorption and desorption without process shut down, and lower pressure drop. Fluidized beds are especially applicable for treating large flow rates, consuming less energy and improving mass and heat transfer (Danielsson and Hudon, 1994; Hamed et al., 2010; Ng et al., 2004; Reichhold and Hofbauer, 1995; Song et al., 2005; Yazbek et al., 2006). The fluidized bed configuration was also declared to be capable of capturing coarse particulate matters in the gaseous dusty streams or slurries like a filter due to the particle – adsorbent contact while fine particulate matters can clog the pores of the adsorbents (Chiang et al., 2000; Geldart and Rhodes, 1986; Khan and Ghoshal, 2000). Fluidized bed configurations are used in the chemical, petroleum, metallurgical, drying, calcination, adsorption, particle sizing, and energy

industries (Kunii and Levenspiel, 1969; Saxena and Vadivel, 1988; Stein et al., 2000).

Many studies have been completed on fluidization and fluidized bed adsorption of different organic and non – organic adsorbates on a variety of catalytic or non – carbonaceous adsorbents. Hamed et al. (2010) investigated the adsorption – desorption characteristics of silica gel for humidity control, finding 20% more humidity capture and faster mass transfer by fluidized bed than fixed bed. Reichhold and Hofbauer (1995) designed Internally circulating fluidized bed to be more compact than fixed bed for continuous adsorption – desorption of CO₂, SO₂, and organic solvent vapors using variety of adsorbents. Fluidization was also performed for VOC capturing on polymeric adsorbent (Song et al., 2005) and on heterogeneous alumina – catalyst adsorbent (Dolidovich et al., 1999). However, very few studies have investigated activated carbon adsorbents in fluidized bed systems.

Activated carbon fluidized beds have been used industrially for capturing VOCs released from large – scale painting operations. After adsorption, the spent GAC was regenerated using hot air and the concentrated VOC – laden air was combusted in thermal oxidizers and used as a fuel source (Wherrett and Ryan, 2004).

Research has shown higher adsorption capacity for fluidized bed systems, when operated under otherwise identical conditions. It is believed that more uniform adsorption occurs during fluidization of the adsorbents (Hamed, 2005; Hamed et al., 2010). In fixed bed adsorption systems, the adsorbent closer to the inlet adsorbs more than the adsorbent near the reactor exit resulting in non – uniform distribution of the adsorbate in the bed, and inefficient use of the adsorbent bed (Hamed, 2002; Pesaran and Mills, 1987).

Spherical activated carbons are ideal for fluidized bed adsorption systems because of their high mechanical strength (low attrition), good fluidity, and low

pressure drop (Romero-Anaya et al., 2010; Wang et al., 2009; Yenisoy-Karakaş et al., 2004).

The minimum fluidization velocity is the lowest gas velocity that fluidizes all adsorbents, and the flooding velocity is the lowest gas velocity that causes the adsorbents exit the reactor. The superficial gas velocity, therefore, should fall between these two parameters. Many researchers have developed equations for calculating superficial gas velocity and other design parameters to be used when constructing fluidized bed adsorption systems (de Vasconcelos and Mesquita, 2011; Delebarre et al., 2004; Kunii and Levenspiel, 1969; Mohanty and Meikap, 2009; Pabiś and Magiera, 2002; Saxena and Vadivel, 1988; Xu and Yu, 1997).

Chiang et al. (2000) found no improvement in VOC adsorption capacity when increasing the gas velocity 1.5 to 2 times over the minimum fluidization velocity. Hamed (2005) found higher adsorption rates at higher superficial gas velocities. In contrast, decreased contact time associated with increased gas velocity may have negative effect on adsorption capacity and kinetics (Roy et al., 2009).

Song et al. (2005) reported that an increase in gas flow rate could result in higher mass transfer with positive effect on adsorption capacity. On the other hand, high gas flow rates could cause higher bed void with negative effect on adsorption capacity. They concluded the later reason to be more effective on adsorption capacity.

Uniform heat distribution in the fluidized bed configuration, avoids the hot spot formation, which happens in fixed bed, and helps adsorption happen in better isothermally developed bed (Hamed et al., 2010).

The impact of humidity on a fluidized bed adsorption system depends on the properties of the adsorbent and the moisture concentration. For example, Reichhold and Hofbauer (1995) suggested that humidity (about 95% in air) during fluidization helps to avoid electrostatic effect while using hydrophobic adsorbents; otherwise it has negative influence on adsorption.

Multistage fluidized beds can reduce the disadvantages of single stage systems by minimizing back-mixing of the phases, arranging flow patterns, decreasing adsorbent attrition, and increasing the system's adsorption efficiency (Varma, 1975). Roy et al. (2009) investigated a multistage fluidized bed system for adsorbing CO₂ on lime and studied the influence of superficial gas velocity, solid velocity, and weir height on removal efficiency. They found the best removal efficiency at high solid flow rates and lower gas velocities because of more gas – solid contact as well as lower solid attrition. Mohanty and Meikap (2009) found that pressure drop and performance through a multistage fluidized bed was similar for all stages (deviation of 2%). They also found that the pressure drop decreases with increasing gas flow rate and decreasing solid flow rate, making fluidized bed more desirable for high gas flow rates than fixed bed.

2.7 Desorption

Desorbing an adsorbate from an adsorbent is intended to restore the adsorption capacity of the adsorbent and to recover the adsorbates for destruction or reuse (Suzuki, 1990). Adsorption and desorption of VOCs on activated carbon can also be a pretreatment process for concentrating the VOCs to facilitate and improve the efficiency of incineration or recovery methods (Khan and Ghoshal, 2000).

Adsorption occurs until equilibrium between the adsorbent and adsorbate is achieved (for a specific temperature and pressure). Reversibly adsorbed compounds can be desorbed by increasing temperature and decreasing pressure (Suzuki, 1990). Other regeneration techniques include adsorbate biodegradation (Scholz and Martin, 1998), acid – base ionization or solvent extraction, competitive adsorption for adsorbate displacement (Yang, 1997), steam regeneration (Kim et al., 2001; Ruhl, 2000), low temperature catalytic oxidation (Sheintuch and Matatov-Meytal, 1999), microwave heating (Ania et al., 2005), electrochemical methods (Wang and Balasubramanian, 2009), and extraction with supercritical fluids (Salvador and Jiménez, 1996). When the mass of adsorbate

adsorbed is equal to the mass desorbed, regeneration is complete (100% regeneration efficiency).

By reducing the total pressure of an adsorbent bed, desorption of the adsorbed compounds occur, which describes pressure swing regeneration (PSR) (Yang, 1997). PSR is generally completed using vacuum on a fixed bed adsorbent (Shonnard and Hiew, 2000).

Temperature swing regeneration (TSR) increases the adsorbent bed temperature using hot gas or heating jackets, coils, or tubes (Yang, 1997). The maximum desorption temperature should overcome the heat of desorption, which is larger than the adsorbate vaporization enthalpy (Popescu et al., 2003). The thermal regeneration depends on thermal stability of the adsorbate and adsorption energy (Liu et al., 1987). TSR is slower and less effective than PSR because of high thermal inertia of adsorbent and lower heat capacity of gases. PSR, however, cannot be applied in fluidized bed systems (Cherbański and Molga, 2009). Moreover, thermal desorption was found to be more efficient than solvent recovery for thermally stable compounds (Ramírez et al., 2010). Nastaj et al. (2006) simulated the combination of TSR and PSR for desorption of VOCs from activated carbon and found that higher desorption efficiencies can be achieved under vacuum in moderate temperatures.

When regenerating a carbon adsorbent at increased temperatures, efforts should be made to maintain the carbon's original structure and adsorption properties. At high temperatures, adsorbates can decompose, polymerize, or react with the carbon surface, possibly resulting in deterioration of the carbon and associated pore blockage (Suzuki, 1990). This effect can be enhanced in the case of chlorine – and sulfur – containing adsorbates (Boulinguez and Le Cloirec, 2010). Gasification of the carbon with steam, CO₂, or oxygen after thermal regeneration can be necessary to recover the adsorption capacity of the activated carbon (Álvarez et al., 2004; Harriott and Cheng, 1988; Sabio et al., 2004; Van Deventer and Camby, 1988). San Miguel et al. (2001) concluded that 5 – 10% burn off by steam gasification is optimal for recovering the adsorption capacity of

the carbon; more burn off might result in production of mesoporous and destruction of micropores.

Activated carbon's shape affects its desorption behavior. AC in powder form (PAC) showed higher heel formation but faster desorption kinetics than GAC due to the improved diffusivity in the smaller particles of PAC (Aktaş and Çeçen, 2006; De Jonge et al., 1996).

Activated carbon with lower catalytic activity, uniform porous structure and uniform adsorption site distribution showed better desorption (Rudling and Björkholm, 1987). For example, desorption can be achieved at lower temperatures for adsorbates adsorbed on mesopores compared to adsorbates adsorbed on micropores (Boulinguez and Le Cloirec, 2010).

Hashisho et al. (2008) and Sullivan et al. (2004) efficiently regenerated activated carbon fiber cloth (ACFC) via electrothermal heating. ACFC's long length fibers can more easily pass electric current to provide heat than PAC or GAC, allowing for higher regeneration efficiencies and adsorbate recovery without a condenser.

Microwave heating is an alternative AC regeneration strategy capable of high regeneration efficiencies with lower energy consumption (Cherbański et al., 2011; Dabek, 2007; Hashisho et al., 2005). Ania et al. (2004) used microwave regeneration to desorb phenols from activated carbon, finding microwave heating as a rapid and useful adsorbent regeneration technique, which does not destruct the porous structure of the adsorbent. Reuß et al. (2002) highlighted the importance of adsorbate and adsorbent properties, including polarity, on microwave regeneration of multicomponent mixtures while Hashisho et al. (2009) studied the effect of ACFC functional groups on microwave heating, concluding that oxygen functional groups decrease microwave heating efficiency.

Subcritical water (300 °C and 120 atm by Salvador and Jiménez (1996) and 350 °C and 150 atm by Rivera-Utrilla et al. (2003)) can efficiently desorb contaminants from activated carbon, though modification of the carbon's

adsorption capacity has been reported. At high temperatures, organics are more soluble in water and decreases in the density, viscosity, and surface tension of water allow for penetration into pores.

Schweiger and LeVan (1993) found thermal regeneration using steam to be more effective than using hot inert gas, because the heat loss through the walls can be compensated by partial condensation of steam to keep the bed temperature constantly high. Furthermore, water can displace the adsorbed compounds. The disadvantage of steam regeneration is the necessity of additional process to separate water from VOCs and also it can cause carbon burn – off (Ahmad and Idris, 2013; Khan and Ghoshal, 2000).

The desorption isotherm and overall adsorption reversibility depends on the concentration of the adsorbate (Suzuki et al., 1978), type of adsorbate and adsorbent, adsorbent pore structure and functional groups (Aktaş and Çeçen, 2006; Fletcher et al., 2006), and operational conditions including temperature and carrier gas velocity (Ramalingam et al., 2012). Irreversibility can be visualized in an adsorption – desorption isotherm as a hysteresis loop (Tamon and Okazaki, 1996; Yonge et al., 1985).

High temperatures achieved during regeneration can decompose the adsorbates or cause chemical reactions between adsorbate species (Maroto-Valer et al., 2006; Salvador and Jiménez, 1996; Wang et al., 2012). Adsorbent pyrolysis can also occur at increased temperatures (Popescu et al., 2003).

Liu et al. (1987) showed that adsorbates larger than octane chemisorb on activated carbon and decompose during thermal desorption. They also explained the desorption role of side chains on aromatics. An aromatic compound with a single alkyl group (lower than C5), like toluene or butylbenzene, showed physisorption while aromatics with alkyl side chains larger than C5 showed decomposition during thermal regeneration.

In conclusion TSR was found as one of the practical techniques to recover the adsorbed compounds and regenerate the adsorbent for reuse. The most

common challenge with desorption is the irreversibility of the adsorption, which might be attributed to the chemisorption, pore diffusion resistance and pore blockage. Thermal desorption can be improved by using different procedures of microwave and electrothermal heating or the combination with PSR instead of conventional heating (e.g. by heating jackets, furnaces, etc.).

CHAPTER 3: MATERIALS AND METHODS

This chapter presents the materials and methods used to fulfill the objectives of this research. The adsorbent and adsorbates are introduced in the materials section followed by the methods used to characterize their physical and chemical properties. Adsorption and desorption experiments, fluidization calculations, characterization tests, thermo – gravimetric analysis, and gas chromatography – mass spectrometry methods are described in the methodology section.

3.1 Materials

3.1.1 Adsorbent

The adsorbent used in this research was microporous beaded activated carbon (BAC) from Kureha Corporation. The BAC has an average particle diameter of 0.71 mm while 99.5% by mass was between 0.60 mm and 0.84 mm. The BAC has a BET surface area, total pore volume, and micropore volume of 1349 m²/g, 0.57 cm³/g, and 0.47 cm³/g, respectively (Jahandar Lashaki et al., 2012b). Pore size distribution of the BAC in Figure 3-1 indicates that the majority of the pores are in the micropore (< 20 Å) range. These properties were determined by nitrogen adsorption (Quantachrome, IQ2MP).

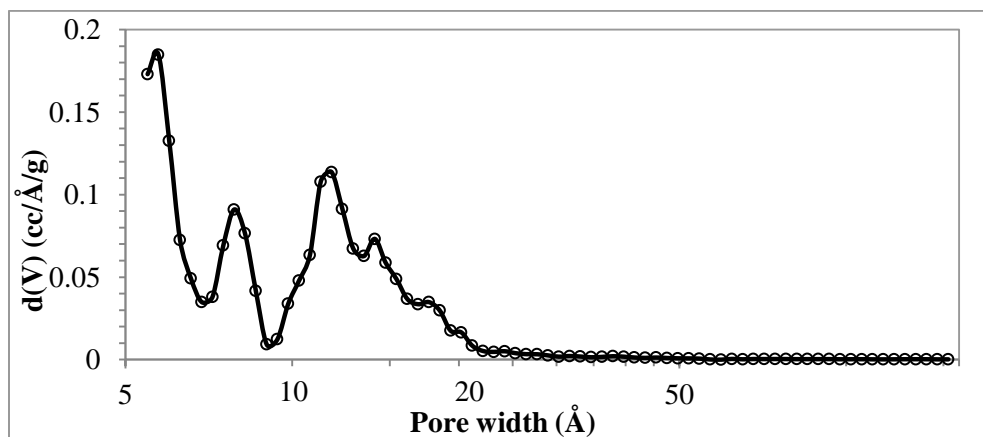


Figure 3-1 Pore size distribution of virgin beaded activated carbon (adapted from (Jahandar Lashaki et al., 2012b))

Elemental analysis of the virgin BAC was determined using x – ray photoelectron spectroscopy (XPS). Table 3-1 presents the XPS results based on atomic and mass concentration.

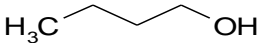
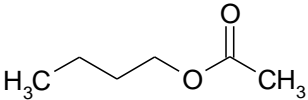
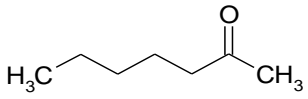
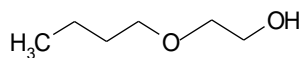
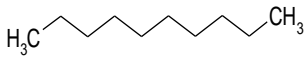
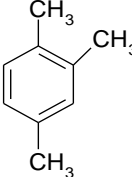
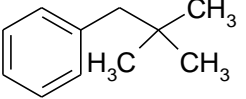
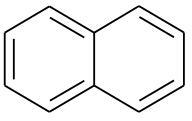
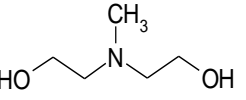
Table 3-1 Elemental composition of virgin BAC by XPS

Element	Mass concentration	Atomic concentration
C	93.2	94.8
O	6.5	5.0
N	0.3	0.2

3.1.2 Adsorbate

Experiments were completed with two different adsorbate streams. First, a single component stream containing 1,2,4 – trimethylbenzene (TMB) was used because TMB has high usage in industrial applications and its bulky structure increases irreversible adsorption, allowing for more accurate comparison of adsorption capacity and heel formation for different configurations. Second, a mixture of nine organic compounds typically emitted from automotive painting operations and representing various functional groups (e.g., alkane, aromatic, ester, alcohol, ketone, polyaromatic hydrocarbon, and amine) was tested for multicomponent adsorption (Table 3-2). To prepare the mixture, equal volumes of each compound were mixed. The density of the mixture was 0.86 g/cm^3 , determined based on the weight of a known mixture volume. The average molecular weight of the components was used as the mixture’s molecular weight (114.5 g/gmol).

Table 3-2 Composition of the VOCs' mixture

Chemical name	Chemical Structure	BP* (°C)	MW* (g/gmol)	Conc.* (ppmv)
n-Butanol (99.9% Fisher scientific)		118	74.1	77
n-Butyl Acetate (>99%, Acros Organics)		126	116.2	54
2-Heptanone (98%, Acros Organics)		151	114.2	51
2-Butoxyethanol (>99%, Acros Organics)		171	118.2	54
n-Decane (99.5%, Fisher Scientific)		174	142.3	36
1,2,4-Trimethylbenzene (98%, Acros Organics)		170	120.2	52
2,2-Dimethyl-propylbenzene (85%, Chemsampco)		186	148.2	41
Naphthalene (>99%, Sigma-Aldrich)		218	128.2	63
Diethanolamine (>98%, Sigma-Aldrich)		271	105.1	73

*BP, MW, and Conc. abbreviated for boiling point and molecular weight, and concentration respectively.

3.2 Methods

3.2.1 Adsorption and regeneration processes

The experimental setup is illustrated in Figure 3-2. The setup consists of an adsorption – desorption reactor, an adsorbate generation system, a gas detection system, a power application module, and a data acquisition and control system (DAC). For both single – and multi – component gas streams, the adsorption – desorption experiments were completed in five consecutive cycles in partial and full adsorbate loading on the BAC in both fixed and fluidized bed configurations during adsorption. Regeneration cycles were completed in fixed bed configuration.

The stainless steel adsorption – regeneration reactor was 20 cm long with inner and outer diameters of 1.44 cm and 1.91 cm, respectively. All experiments were performed with 7 ± 0.2 g of dry, virgin BAC. The BAC was dried in a laboratory oven for 24 h at 150 °C and cooled in a desiccator prior to each experiment. The BAC bed height was 8 cm in the fixed bed configuration while the bed height increased during fluidization. Glass wool was used at the bottom and top of the carbon bed as a support for the fixed bed configuration. Glass wool was used at the bottom of the fluidized bed and a stainless mesh screen was used at the top of the reactor to prevent the adsorbent beads from exiting through the top of the reactor during fluidization. During adsorption, the air flow (10 SLPM) was from bottom to top of the reactor with the same flow rate for both fixed and fluidized bed configurations. The fluidization calculations are given in section 3.2.5.

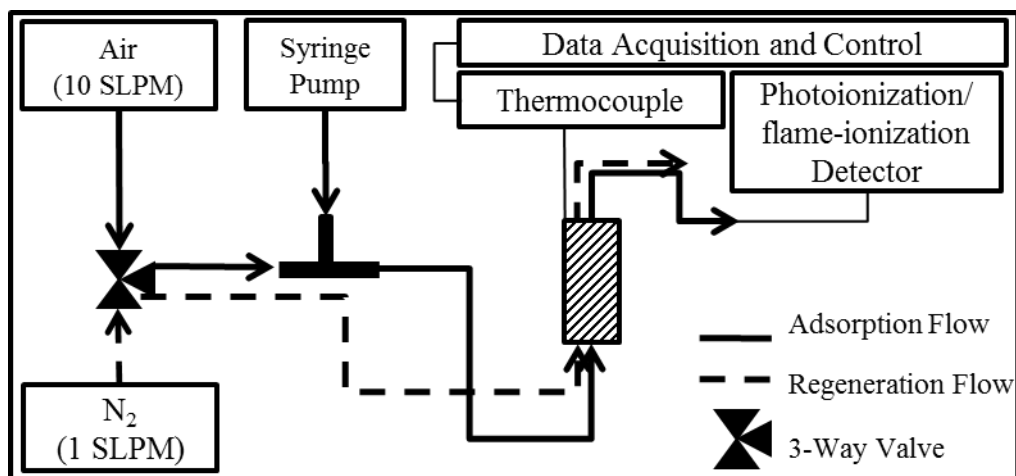


Figure 3-2 Schematic of the adsorption – desorption setup

Adsorbate was injected using a syringe pump (New Era, NE-300) into a 10 standard liter per minute (SLPM) at 1 atm and 25 °C of filtered air. A compressed air filter (Norman Filter Co.) was used to remove water and hydrocarbons from the air stream. The air flow rate was controlled at 10 SLPM using a mass flow controller (Alicat Scientific). The syringe pump injection rate was adjusted to maintain an inlet adsorbate concentration of 500 ppmv for all the experiments. The injection rate was calculated based on the ideal gas law using the adsorbates' density and molecular weight. The inlet and outlet organic concentrations were determined with a photoionization detector (PID) (Minirae 2000, Rae Systems). Contamination of the PID lamp may occur due to continuous contact with high boiling point organic compounds present in the organic mixture, and for this reason, intermittent measurement of the organic concentrations were completed and a flame – ionization detector (FID) was used in case of mixture (Baseline Mocon, Series 9000). The FID used ultrahigh purity (grade 5.0) hydrogen gas with flow rate of 35 cc/min and compressed air as a combustion gas with flow rate of 175 cc/min.

The PID (for single component) and FID (for mixture) were calibrated before each experiment. The inlet adsorbate concentration was stabilized before the flow was directed towards the reactor. Clean air was used for zero calibration and the steady flow of the adsorbate was used as the span point, which was 500

ppmv for all tests. Calibration was performed with the same flow rate as the one used during adsorption to reduce errors in concentration measurements. Adsorption stopped when the BAC was fully loaded in the complete loading experiments (180 min for 1,2,4 – trimethylbenzene and 240 min for VOC mixture). For partial loading tests, adsorption stopped after 90 min for the 1,2,4 – trimethylbenzene adsorbate and 120 min for the VOC mixture adsorbate. The breakthrough time and saturation time were determined using the PID and FID for the single – and multi – component gas streams, respectively. In this research, the times in which the effluent concentration was 1% and 99% of the inlet concentration, were used as breakthrough and saturation time, respectively.

Regeneration was completed using thermal regeneration. Heat was applied using a heating tape (Omega) wrapped around the reactor. A solid – state relay controlled power application to the heating tape. Insulation tape (Omega) covered the heating tape to minimize heat loss. A 0.9 mm OD (outer diameter) type K thermocouple (Omega) inserted into the center of the fixed height of BAC column was used to measure and control the temperature at 25 °C and 288 °C during adsorption and regeneration, respectively. Temperature control was performed using a data acquisition and control (DAC) system consisting of a LabVIEW program (National Instruments) and a data logger (National Instruments, Compact DAQ) equipped with analog input and output modules. The data logger was interfaced to the thermocouple and the solid state relay. The temperature during regeneration was controlled by applying power using the DAC system and a proportional – integral – derivative algorithm until the set point temperature was reached.

High purity (grade 4.8) nitrogen (1 SLPM) was used during regeneration to purge oxygen from the bed and carry desorbed compounds. Desorption tests were performed at 288 °C for 3 h followed by 50 min cooling with continuous nitrogen purging of the bed.

Adsorption and desorption amounts were determined using mass balances. The reactor was weighed using a balance (Mettler Toledo, MS603S) before and

after adsorption and desorption to calculate the adsorption capacity of the BAC achieved in each adsorption experiment and the amount of irreversible adsorption or heel formation after desorption, according to Equations 3-1 and 3-2, respectively.

$$\text{Adsorption Capacity (\%)} = \frac{(W_{A.A} - W_{B.A})}{W_{BAC}} \times 100 \quad 3-1$$

$$\text{Heel formation (\%)} = \frac{(W_{A.D} - W_{B.D})}{W_{BAC}} \times 100 \quad 3-2$$

Where, $W_{B.A}$ and $W_{A.A}$ are the weight of the reactor filled with BAC before and after adsorption, respectively; $W_{B.D}$ and $W_{A.D}$ are the weight of the reactor before and after desorption process, respectively. W_{BAC} represents the weight of virgin dried BAC used. The effect of mixture condensation on glass wool on adsorption capacity was also considered in the results using a blank test.

For consecutive adsorption – regeneration cycles, the weight of virgin carbon used at the beginning of the first cycle was used as W_{BAC} and the weight of the reactor after each desorption step was substituted as the before adsorption reactor weight for the next cycle. Cumulative heel formation after five adsorption – desorption cycles was calculated using Equation 3-3.

$$\text{Cumulative heel formation (\%)} = \frac{W_{A.D}(\text{last cycle}) - W_{B.A}(\text{1st cycle})}{W_{BAC}} \times 100 \quad 3-3$$

3.2.2 Characterization tests

BAC samples were characterized using nitrogen adsorption (IQ2MP, Quantachrome) at 77 K with relative pressures from 10^{-6} to 1. About 30 to 40 mg of sample was degassed at 120 °C for 5 h to remove moisture and organics. BET surface area and micropore volume were obtained using relative pressure ranges of 0.01 – 0.07 and 0.2 – 0.4, respectively. Surface area and micropore volume were determined using the BET equation and V – t method, respectively. The pore size distribution and total pore volume were obtained from the nitrogen adsorption

isotherms using density functional theory (DFT). The mesopore volume was calculated from subtracting the micropore volume from total pore volume, which assumed negligible macroporosity.

All spent BAC samples were characterized after five cycles of adsorption and desorption to determine the effect of adsorption bed configuration on pore size distribution and surface area of the adsorbents.

3.2.3 Thermo – gravimetric analysis

Thermo – gravimetric analysis (TGA) was performed to determine the amount of accumulated adsorbate (heel formation) on BAC after five adsorption – regeneration cycles, and to determine the heel formed on loaded BAC located in different parts (top, middle, and bottom) of the reactor. This is done after regeneration to identify the distribution of adsorbate heel throughout the BAC bed using both fixed and fluidized bed configurations.

Thermo – gravimetric analyses were completed using TGA (TGA/DSC 1, Mettler Toledo). The samples were heated at 20 °C/min in 50 standard cubic centimeters per minute (SCCM) of N₂ (Praxair, grade 4.8). The temperature increased from 30 °C to 120 °C then was stable at 120 °C for 15 min to remove moisture. Temperature was then increased to 288 °C, the regeneration set point temperature, and stabilized for 30 min. Temperature was then increased again to 530 °C and stabilized for another 30 min to desorb strongly adsorbed adsorbates from BAC. The diagram for this heating program is shown in Figure 3-3.

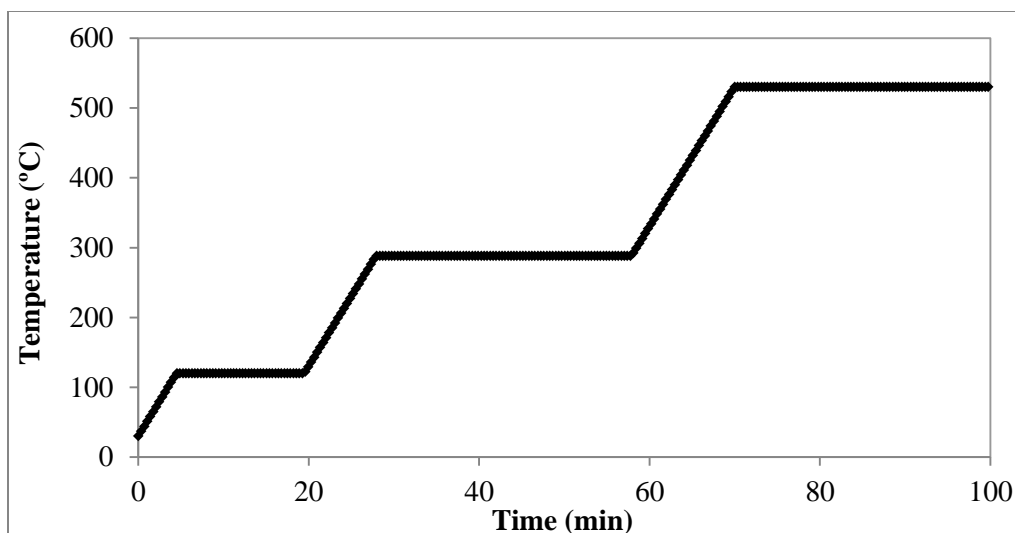
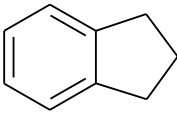


Figure 3-3 TGA temperature program diagram

3.2.4 Gas chromatography – mass spectrometry analysis

GC – MS was used to understand the adsorption differences between fixed bed and fluidized bed configurations. The multi-component adsorbates mixture was used for these tests (Table 3-2) with naphthalene replaced with indan and diethanolamine removed. These compounds were removed because naphthalene can condense in the GC – MS column and diethanolamine cannot be detected by GC – MS (Wang et al., 2012). Table 3-3 describes the physical and chemical properties of indan. The mixture was prepared using the same concentration of individual components (62.5 ppmv) and an overall adsorbate concentration of 500 ppmv.

Table 3-3 Indan physical and chemical properties

Chemical name	Chemical Structure	BP (°C)	MW (g/gmol)
Indan (95%, sigma-Aldrich)		176	118.2

Effluent gas samples were collected periodically (every 15 min) with 250 mL Tedlar bags (Saint Gobain Chemware) and injected immediately into a GC –

MS (Agilent Technologies model 7890A GC interfaced to 5975C inert MSD with Triple-Axis Detector) detector.

The GC was equipped with a DB-1 advanced fused – silica capillary column that is 60 m long with a 0.32 mm diameter and 3 μm film thickness (Agilent J&W). The injected sample was carried through the column using helium with a flow rate of 2.6 mL/min. The injection volume was 1 mL and the split ratio was 5 – 10:1 for gas analyses. The injection port temperature was 260 $^{\circ}\text{C}$ and the oven temperature was ramped at 30 $^{\circ}\text{C}/\text{min}$ from 80 to 260 $^{\circ}\text{C}$ and held for up to 13 min (Wang et al., 2012).

The total concentration of the effluent gas stream was determined by summing all component concentrations detected by GC – MS and was compared to the concentration monitored using FID. The GC – MS was calibrated using the inlet concentration of each adsorbate (62.5 ppmv) before starting adsorption. The FID was calibrated with the generated inlet stream (500 ppmv) as the span point and clean air as the zero point calibration. The adsorption experiments were performed for 390 minutes for full loading of the BACs.

3.2.5 Fluidization calculation

The behavior of a fluidized bed depends on the properties of the gas and solid phases. The parameters needed to determine the gas velocity are the minimum fluidization velocity (u_{mf}) and minimum fluidization porosity (ϵ_{mf}). The minimum fluidization porosity and minimum fluidization velocity were calculated using Equations 3-4 and 3-5, respectively. These equations are applicable when Reynolds number (Re) is < 10 . The Reynolds equation is also included in Equation 3-6 (Broadhurst and Becker, 1975).

$$\epsilon_{mf} = 0.586\psi^{-0.72} \left(\frac{\mu_g^2}{\rho_g \eta d_p^3} \right)^{0.029} \left(\frac{\rho_g}{\rho_c} \right)^{0.021} \quad 3-4$$

$$u_{mf} = \frac{(\psi d_p)^2}{150\mu_g} \eta \frac{\epsilon_{mf}^3}{1 - \epsilon_{mf}} \quad 3-5$$

$$Re = \frac{\rho_g u_g d_p}{\mu_g} \quad 3-6$$

The superficial gas velocity (u_g) was calculated using Equation 3-7, and is based on an adsorption reactor inner diameter (d) of 1.44 cm and an air flow rate (Q) of 10 SLPM. For Reynolds number > 10 , Equation 3-8 (Ergun equation) should be used to obtain porosity of the bed (Kunii and Levenspiel, 1969).

$$u_g = \frac{Q}{\pi d^2/4} \quad 3-7$$

$$\eta(1 - \varepsilon) = \rho_g u_g^2 \left(\frac{150(1 - \varepsilon)}{Re\psi} + \frac{7}{4} \right) \frac{1 - \varepsilon}{\psi d_p \varepsilon^3} \quad 3-8$$

Table 3-4 describes calculated fluidized bed parameters based on the BAC and experimental conditions used in this work. The BAC is assumed to be spherical. Gas properties were assumed to be the same as air, since the adsorbates' concentration ($\approx 5 \times 10^{-3}$ L/min) was low compared to the air flow rate (10 SLPM).

Table 3-4 Equations' parameters description and value

Parameter	Description	Value	Unit
ψ	Sphericity	1	-
μ_g	Gas phase (air) viscosity	1.86×10^{-5}	Kg/m.s
ρ_g	Gas phase (air) density	1.09	Kg/m ³
ρ_c	BAC density	850	Kg/m ³
η	$g(\rho_c - \rho_g)$	8327.84	Kg/m ² s ²
d_p	BAC particles diameter	0.71	mm

The fluidization maximum velocity was calculated using Equation 3-9 (Kunii and Levenspiel, 1969).

$$u_t = \left(\frac{1.78 \times 10^{-2} \eta^2}{\rho_g \mu} \right)^{\frac{1}{3}} (d_p) \quad 0.4 < \text{Re} < 500 \quad 3-9$$

Since Reynolds number was 48, the porosity of the bed was 0.78, calculated using Equation 3-8. The fluidization velocity must be between the minimum and maximum velocity, as is the case for this setup. The experimental system had a minimum fluidization velocity of 0.07 m/s (Equation 3-5), minimum fluidization porosity of 0.32 (Equation 3-4), maximum fluidization velocity of 2.79 m/s (Equation 3-9), and superficial gas velocity of 1.02 m/s, allowing for fluidization without flooding the bed.

Pressure drop through the bed was calculated considering the porosity obtained during fluidization (Equation 3-10). According to the equation, pressure drop over the fluidized bed was 18.32 Pa/cm of the adsorbent column.

$$\Delta P/h = (\rho_c - \rho_g)g(1 - \varepsilon) \quad 3-10$$

CHAPTER 4: RESULTS AND DISCUSSION

4.1 Adsorption and desorption processes

Adsorption and desorption experiments were completed in five consecutive cycles to find the effects of the adsorption bed configuration on both adsorption and desorption processes. Results are discussed in this section in terms of breakthrough curves, adsorption capacities, and desorption performance.

4.1.1 Breakthrough profiles

Breakthrough curves depict effluent VOC concentrations during adsorption, as a function of time. For the results presented herein, figures include breakthrough curves for five consecutive adsorption cycles. The breakthrough curve highlights the time when emissions start and when the BAC becomes fully loaded. As mentioned in Section 3.2, all the breakthrough times discussed in this chapter are based on the effluent concentration reaching 1% of the inlet concentration. Adsorption capacity for each cycle can be found by integrating the area above the breakthrough curve (and below the inlet VOC concentration) during adsorption. Adsorption cycles were completed in both fixed bed and fluidized bed adsorption configurations using a single component adsorbate and a mixture of adsorbates.

4.1.1.1 Single component adsorption

Figure 4-1 includes the breakthrough curves during five consecutive adsorption cycles for (a) fixed bed and (b) fluidized bed configurations. Both configurations consisted of 7 ± 0.2 g of BAC.

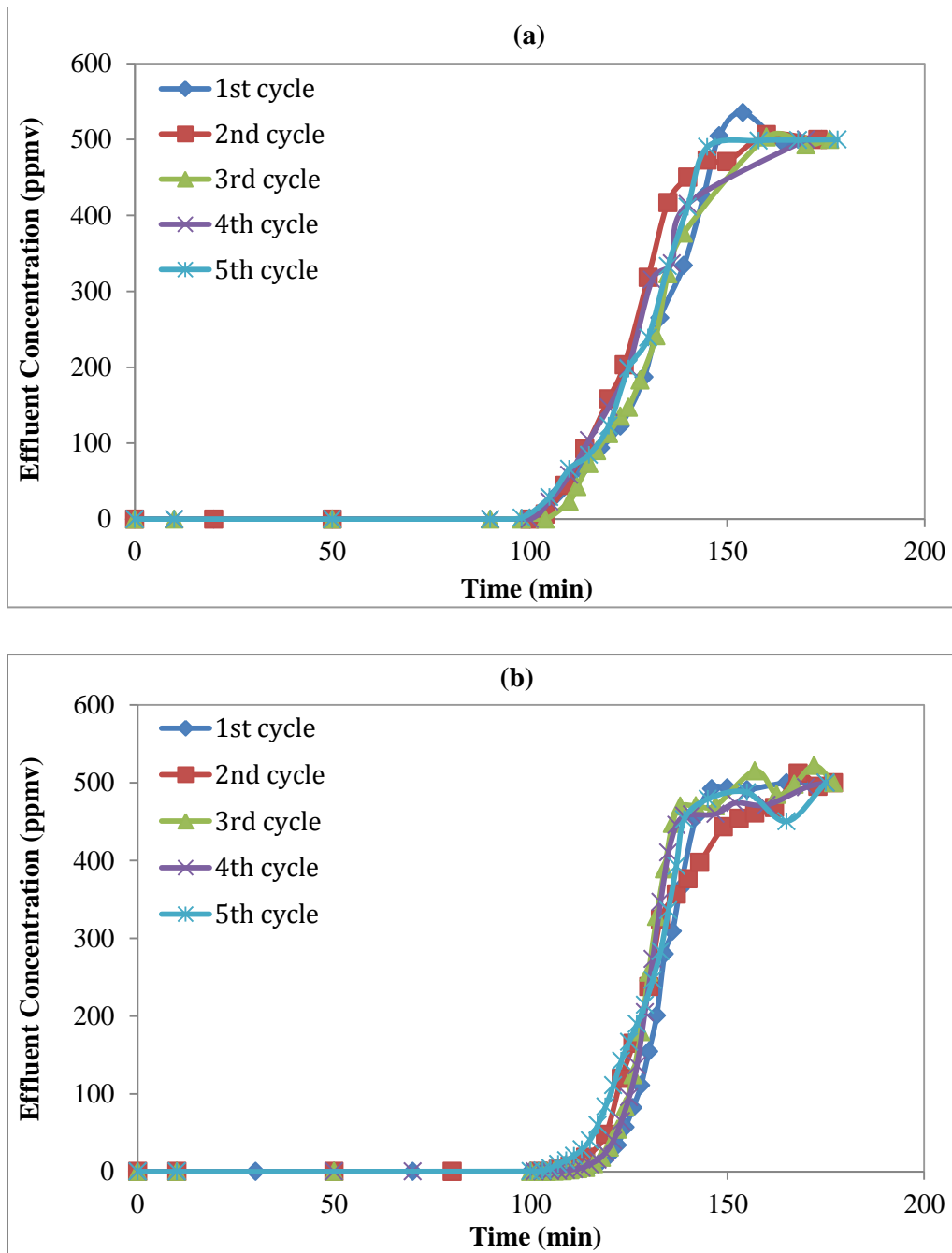


Figure 4-1 Breakthrough curves for five consecutive adsorption cycles of 1,2,4 – trimethylbenzene on BAC using different adsorption bed configurations (a) Fixed bed and (b) Fluidized bed

Breakthrough times for adsorption of 1,2,4 – trimethylbenzene on BAC for fixed bed and fluidized bed configurations differ about 13 min for the fixed bed occurring sooner. For the first cycle, breakthrough occurs after 101 and 114

min using fixed and fluidized beds, respectively. BAC was completely loaded after 180 min for both configurations. It can be concluded that the adsorption bed configuration influenced the breakthrough time for the single adsorbate scenario. The fluidized bed configuration, however, showed a sharper breakthrough curve than the fixed bed configuration, which is attributed to improved mass transfer and mixing achieved by fluidization. The slope of the breakthrough profile was determined using the throughput ratio (TPR), which is the ratio of the breakthrough time to the time when effluent concentration was 50 % of the influent concentration. For the single component adsorbate, the average TPR for the 5 cycles was 0.78 ± 0.02 and 0.88 ± 0.03 for fixed bed and fluidized bed configurations, respectively. These results are consistent with the literature; Ng et al. (2004) and Song et al. (2005) also found sharper breakthrough curves using fluidized bed configurations for the adsorption of methanol and isobutane on ZSM – 5 and toluene on polymeric adsorbent, respectively. Calculated adsorption capacities based on the above breakthrough curves were 42.7% and 43.9% by weight for fixed bed and fluidized bed adsorption, respectively, a 2.8% difference. These adsorption capacity results were reproducible, as described in section 4.1.2 with standard deviations.

Both configurations demonstrated negligible change in breakthrough times for consecutive adsorption cycles. This supports that adsorption of 1,2,4 – trimethylbenzene is reversible and complete regeneration and adsorption capacity recovery are achieved during thermal desorption. Desorption results are discussed in more detail in sections 4.1.3.

1.1.1.1 Multicomponent adsorption

Since most emissions from industrial sources contain many organic compounds with different functional groups and physical properties, a VOC mixture containing nine organic compounds (described in Table 3-2) was used as a multicomponent adsorbate. The adsorption capacity of BAC for the VOC mixture, the effect of configuration on adsorption and desorption, and competitive

adsorption were investigated. Figure 4-2 demonstrates the breakthrough curves obtained using the FID during adsorption.

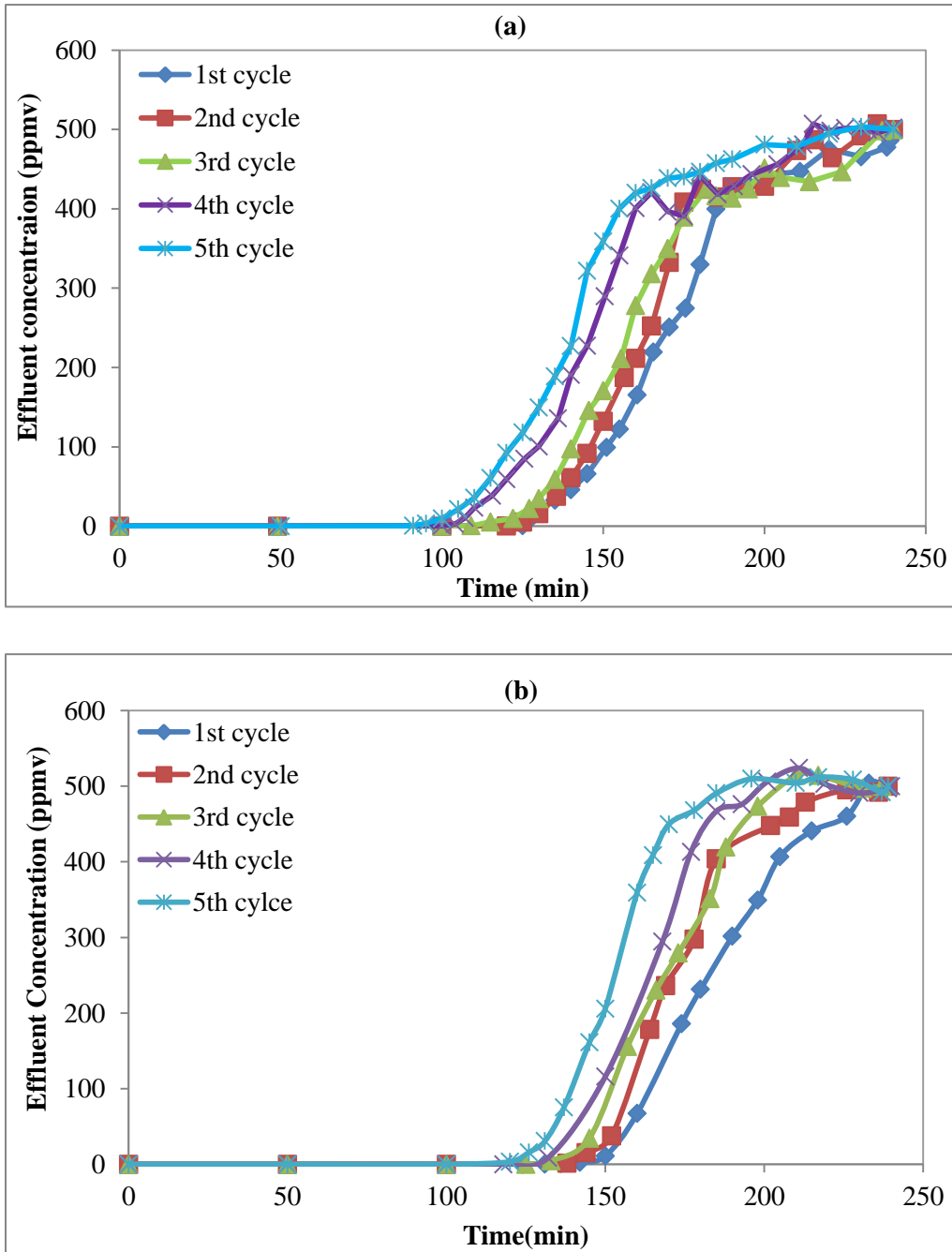


Figure 4-2 Breakthrough curves for five consecutive adsorption cycles of a VOC mixture on BAC using different adsorption bed configurations (a) Fixed bed and (b) Fluidized bed

Once again, breakthrough times were longer and sharper for the fluidized bed than the fixed bed, indicating better mass transfer. Breakthrough time for the first cycle was 130 and 144 minutes for the fixed and fluidized beds, respectively. Calculated average TPRs were 0.73 ± 0.03 and 0.79 ± 0.01 for fixed bed and fluidized bed, respectively.

The 5th cycle breakthrough times showed 26% and 16% decrease in from the 1st cycle breakthrough time for the fixed and fluidized bed, respectively. This decrease demonstrates incomplete recovery of the adsorption capacity during consecutive cycles occurring more in case of fixed bed configuration. The detailed regeneration results are discussed in Section 4.1.3.

Adsorption capacity for the multi – component system cannot be calculated from breakthrough curves because of experimental errors such as adsorbate condensation on glass wool and tubing, the increase of the average density and molecular weight of the adsorbed species during adsorption, and the FID different response factors for different components in the mixture. The concentration profiles for each individual compound are discussed in Section 4.4.

4.1.2 Adsorption capacity

The adsorption capacity of virgin BAC was calculated using mass balance (Equation 3-1) for all experiments (Tables in Appendix A for 1,2,4 – trimethylbenzene and Appendix C for VOC mixture) and the average values were reported. Adsorption capacities for fixed and fluidized bed adsorption configurations were also compared in both partial and full loading. Based on experiments, for full loading tests, adsorption stopped after 180 minutes for 1,2,4 – trimethylbenzene and 240 minutes for the adsorbate mixture. Stopping adsorption after 90 minutes for 1,2,4 – trimethylbenzene and 120 minutes for VOC mixture was tested and shown to be an appropriate time to avoid emissions during the first cycle of partial loading tests. The same criterion was used to determine adsorption time during subsequent cycles. Figure 4-3 compares adsorption capacities for all tested scenarios.

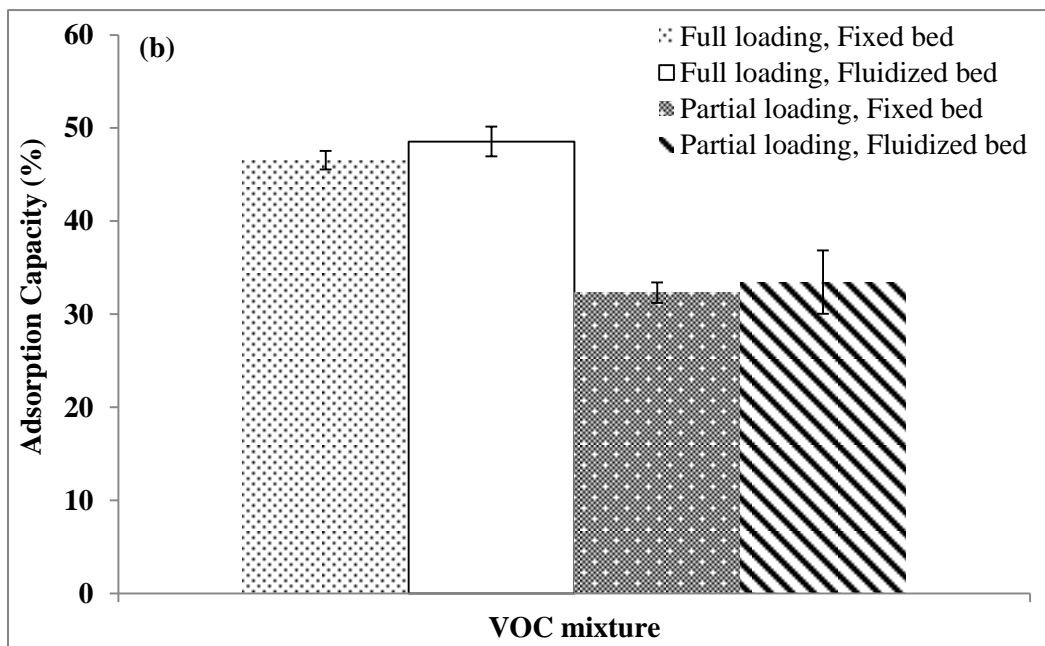
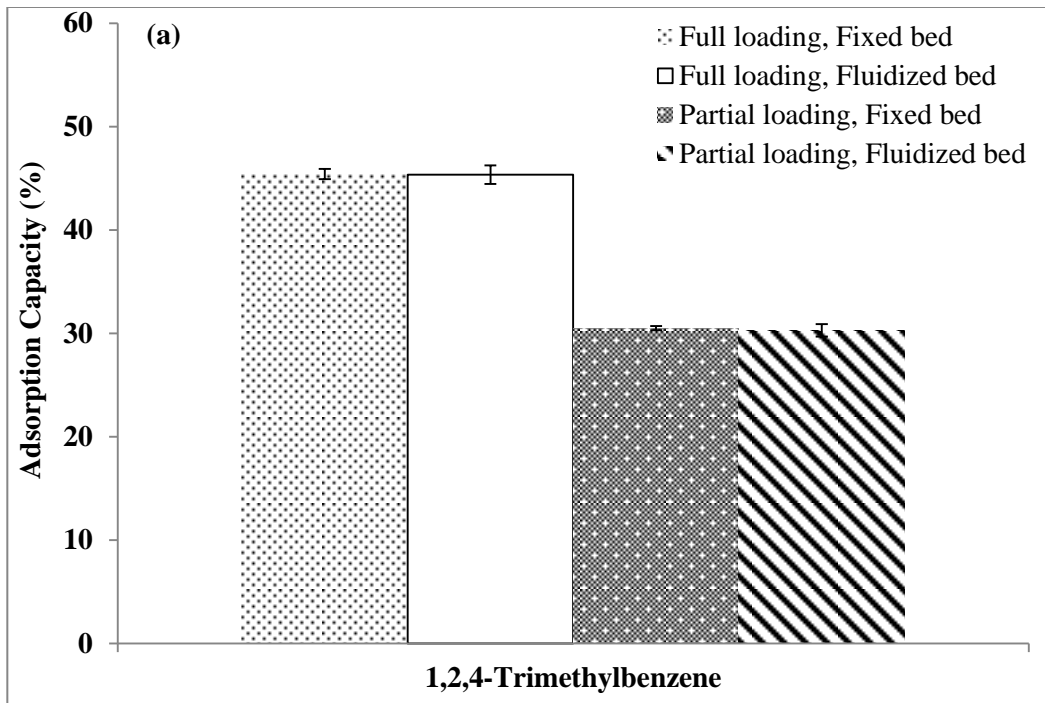


Figure 4-3 Comparing the adsorption capacity of the virgin BAC for (a) 1,2,4 – trimethylbenzene and (b) VOCs’ mixture in different configurations accompanied by the standard deviation error bars

Adsorption capacities obtained for full loading of BAC with 1,2,4 – trimethylbenzene using fixed and fluidized beds were both 45.4% by weight with

standard deviations of 0.5% and 0.9%, respectively. Adsorption capacities were $30.5\% \pm 0.2\%$ and $30.3\% \pm 0.6\%$ for partial loading of the fixed and fluidized beds, respectively. Therefore, it can be concluded that the configuration did not have influence on the adsorption capacity of the single component.

Adsorption capacities obtained for full loading with the VOC mixture adsorption were $46.6\% \pm 1.0\%$ and $48.6\% \pm 1.6\%$ for fixed and fluidized bed configurations, respectively. The capacities were $32.3\% \pm 1.1\%$ and $33.5\% \pm 3.4\%$ for partial loading of the fixed and fluidized beds.

Almost similar adsorption capacities in full loading experiments demonstrate that both configurations were capable of using virgin BAC capacity but the difference in the breakthrough curves demonstrate different adsorption kinetics for fixed bed and fluidized bed configurations.

In partial loading experiments of the virgin BAC, similar amount of the adsorbate was entered into the adsorbent bed for a specific period of time while no emission of adsorbates were detected from the reactor effluent in both configurations, thus, the virgin BAC were able to adsorb all the adsorbates and similar adsorption capacities were expected.

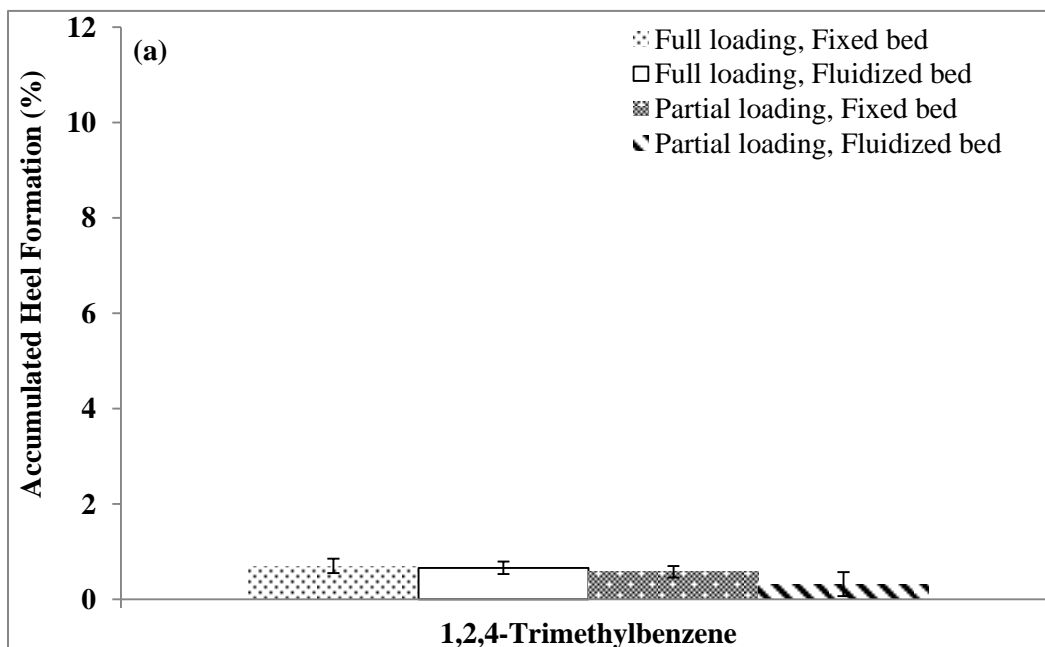
As zero emission of the pollutants is the purpose of the adsorption in industry, longer breakthrough times and sharper breakthrough curves for the fluidized bed allows for increased adsorption before any emission of the pollutants. Adsorption capacities obtained when the effluent organic concentration reached 1% of the inlet concentration were 38.4% (adsorption stopped after 122 minutes using fluidized bed) and 33.7% (100 minutes using fixed bed) for 1,2,4 – trimethylbenzene and 38.6% (150 minutes using fluidized bed) and 36.5% (133 minutes using fixed bed) for the mixture. This indicates that higher pollutants removal can be achieved in fluidized bed configuration before the need to regenerate the adsorbents.

In conclusion, the adsorption capacities were not influenced by the adsorption bed configuration for both 1,2,4 – trimethylbenzene and mixture. The

results confirm that the fluidized bed configuration is capable of capturing pollutants as well as fixed bed with better mass transfer, and shorter MTZ (Chiang et al., 2000)

4.1.3 Regeneration efficiency

Regeneration efficiency is the fraction of adsorbed adsorbates desorbed during regeneration. Adsorbate that is not removed during regeneration corresponds to heel formation. Higher heel might be attributed to irreversibility of the adsorption process or diffusive mass transfer resistance. Irreversible adsorption is mainly due to chemisorption and oligomerization (Aktaş and Çeçen, 2007). Oligomerization has only been shown for aqueous – phase phenol adsorption (Yan and Sorial, 2011), and so irreversible adsorption in this work might be due to chemisorption or pore blockage by bulky molecules. Figure 4-4 shows the accumulated heel after five cycles for all experiments completed in full and partial loading of the adsorbent (Equation 3-3) (Tables in Appendix B for 1,2,4 – trimethylbenzene and Appendix D for VOC mixture).



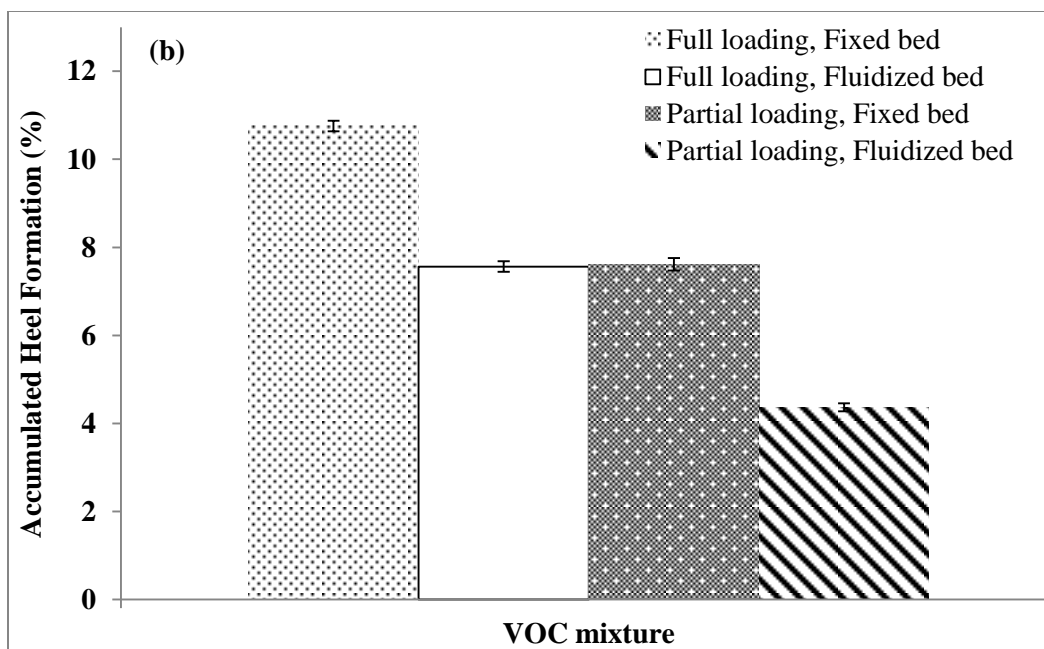


Figure 4-4 Comparing the cumulative heel formation after five cycles adsorption-desorption of (a) 1,2,4 – trimethylbenzene and (b) VOC mixture on BAC in fixed bed and fluidized bed adsorption configurations accompanied by standard deviation error bars

All the regeneration experiments were completed under the same conditions, with nitrogen as carrier gas with flow of 1 SLPM, 288 °C, and fixed bed configuration. The temperature profile for both fixed bed and fluidized bed adsorption configurations (Figure 4-5) shows identical heating during the fixed bed desorption (of the adsorbents loaded by fluidized bed and fixed bed adsorption configuration).

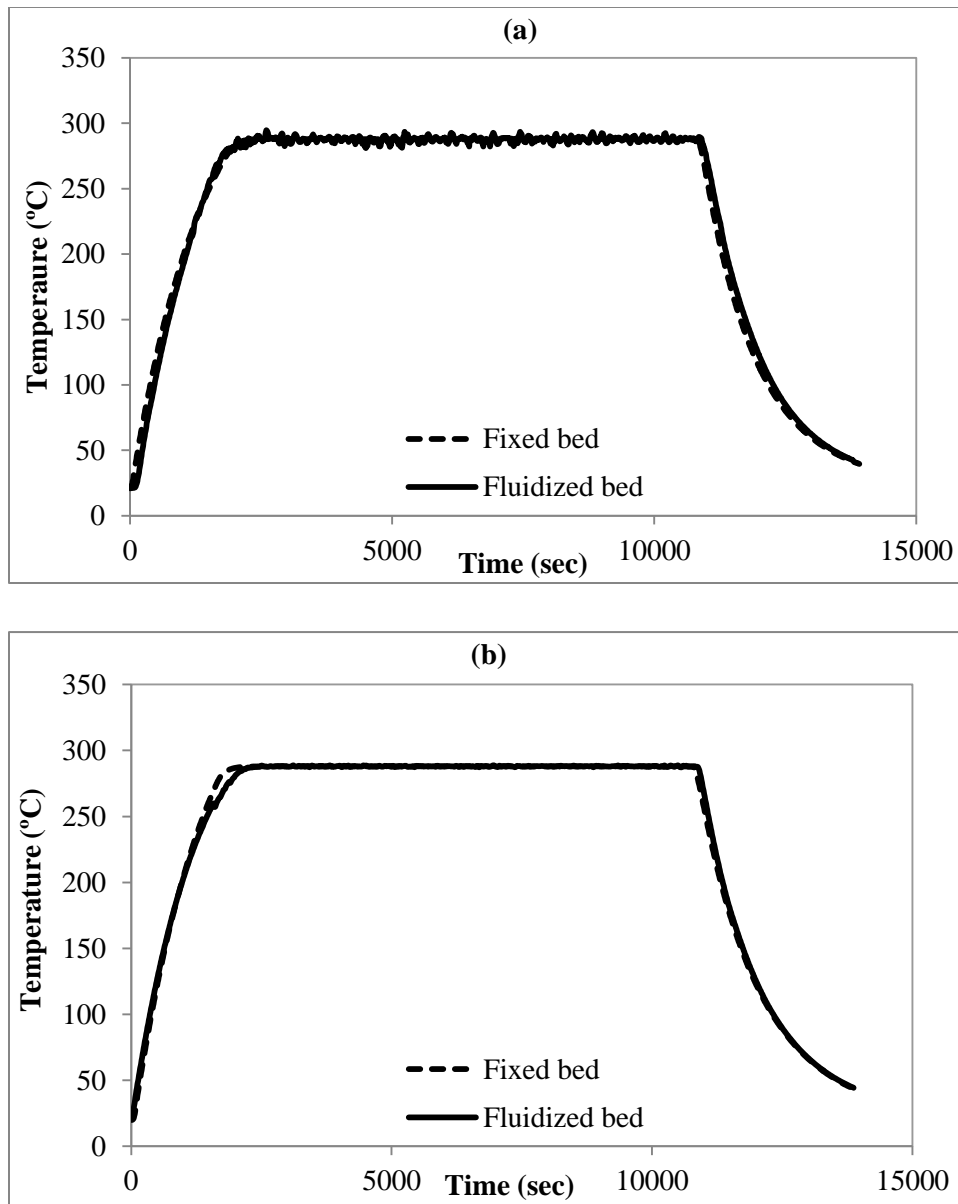


Figure 4-5 Temperature profile during fixed bed desorption of (a) 1,2,4 – trimethylbenzene (b) VOC mixture from BAC. The adsorbents were loaded by fixed bed and fluidized bed adsorption configuration.

In addition to the temperature profiles, Table 4-1 shows that energy consumption was similar for all experiments performed in both fixed bed and fluidized bed adsorption configurations. Figure 4-5 and Table 4-1 indicates that the same heating conditions were used for the regeneration of the adsorbents loaded in fixed and fluidized bed configurations.

Table 4-1 Average energy consumption (in MJ) for all the experiments during 3-hour regeneration heating

	VOC mixture	1,2,4 – Trimethylbenzene
Full loading, Fixed bed	83.8	91.4
Full loading, Fluidized bed	84.0	92.9
Partial loading, Fixed bed	82.3	93.5
Partial loading, Fluidized bed	84.5	89.3

According to Figure 4-4 (a), cumulative heel formation for the single component adsorbate after five cycles in full and partial loading was less than 1% by weight for both configurations. Differences in heel formation are within the experimental error (as indicated by the standard deviation).

Heel formation for full loading of the adsorbate mixture was 10.8% and 7.6% for fixed and fluidized bed configurations, respectively. Cumulative heel was 7.6% and 4.4% for partial loading in fixed and fluidized bed configurations, respectively. The standard deviation for cumulative heel for experiments with the adsorbate mixture was approximately 0.1%.

The fixed bed configuration caused 30% to 42% more heel formation than the fluidized bed configuration with the adsorbate mixture for both partial and full loading. Therefore, fluidization during adsorption was found to yield lower irreversibility than the fixed bed adsorption procedure. It can be concluded that fluidization during adsorption decreases the causes of irreversible adsorption. The BAC samples thermo – gravimetric analysis and also micropore analysis were completed to support the mass balance results. These results are given in sections 4.2.1 and 4.2.2, respectively.

The non – uniform adsorption in the fixed bed in both partial and full loading of the adsorbents might be the reason for the heel differences. As no discernible difference was observed in single component heel formation, therefore, the combination of non – uniformity of the fixed bed and competitive

adsorption in case of the mixture might be responsible for higher heel formation in this configuration. To find out the effect of non – uniformity during adsorption on desorption and also the effect of competitive adsorption, TGA and GCMS experiments were completed and described in sections 4.3 and 4.4 in details. Lower heel formation for partial loading in comparison to full loading is expected due to less adsorbate captured by the BAC.

4.2 Characterization tests

Characterization tests were performed on spent BAC samples after five cycles of adsorption and regeneration to verify the results obtained by mass balance. Thermo – gravimetric analysis and pore size analysis were performed for this purpose.

4.2.1 Thermo – gravimetric analysis (TGA)

Spent BAC samples were analyzed with thermo – gravimetric methods after five cycles of partial and full loading of 1,2,4 – trimethylbenzene and the VOC mixture in both fixed and fluidized bed adsorption configurations and fixed bed regeneration. The samples were heated to 530 °C in TGA to remove the remaining strongly adsorbed compounds after regeneration from BAC (Jahandar Lashaki et al., 2012b). Therefore, total weight loss in TGA experiments is expected to be comparable to the amount of accumulated adsorbate, or heel formation. The samples' weight loss versus temperature is demonstrated in Figure 4-6. Results for fixed bed and fluidized bed are included in the same figure for each of the adsorbate streams to allow for easy comparisons.

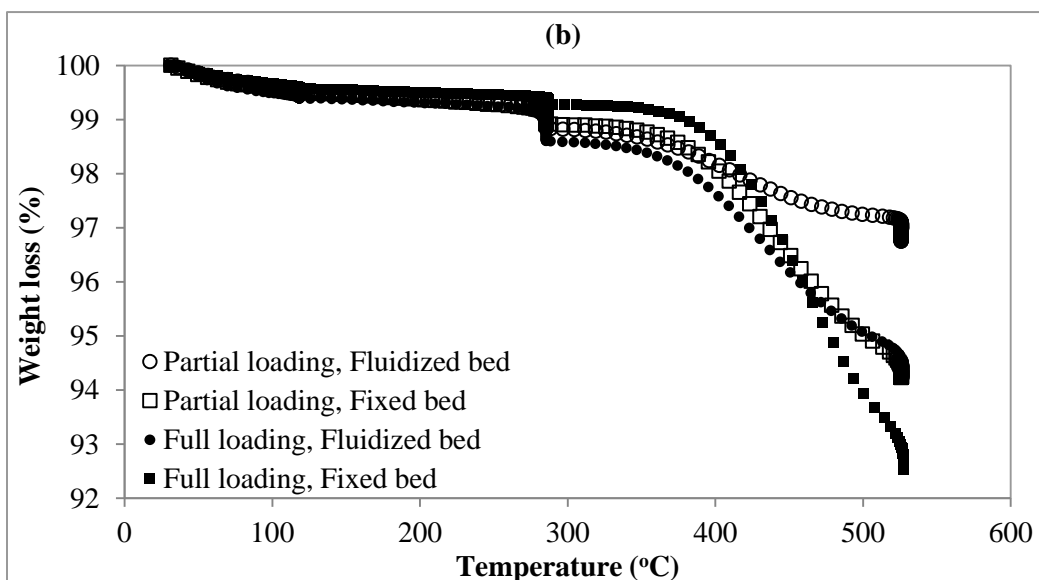
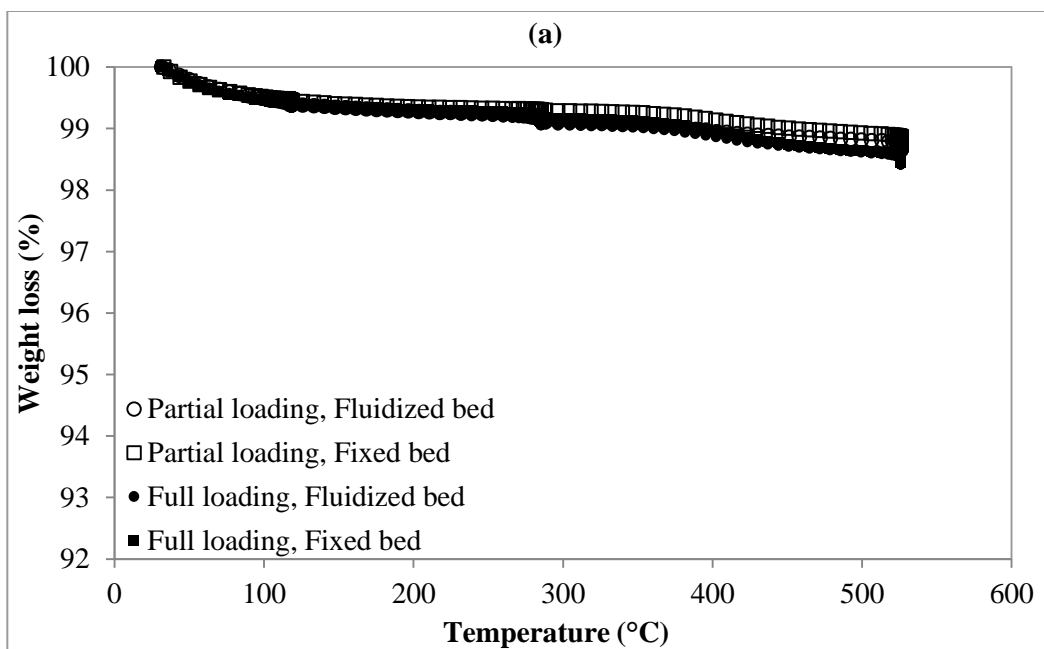


Figure 4-6 TGA results for the 5th cycle regenerated BAC samples loaded previously with (a) 1,2,4 – trimethylbenzene and (b) VOC mixture

Figure 4-6 (a) confirms the small effect of adsorption bed configuration on irreversible adsorption of 1,2,4 – trimethylbenzene on BAC. The weight loss percentage (1.2% – 1.6%) was similar for all samples loaded with the single adsorbate. Figure 4-6 (b) shows higher weight loss for the fixed bed regenerated BAC samples loaded both partially and fully with the VOC mixture. This can be

attributed to more accumulated adsorbates on BAC that could not be desorbed at 288 °C. Presence of bulky structured molecules (with high molecular weight and boiling point) might be responsible for the heel formation of the mixture on BAC, which could not be desorbed completely due to their high affinity to the adsorbent and pore diffusion (Jahandar Lashaki et al., 2012b; Wang et al., 2012). More accumulated adsorbate for the fixed bed samples might be attributed to displacement of light compounds with heavier ones, as well as re – adsorption of desorbed lighter compounds on virgin adsorbents in the upper parts of the reactor which resulted in gradual increase of the effluent concentration demonstrated by breakthrough curves and the lighter compounds effluent concentration depicted in GCMS results. The non – uniform distribution of the adsorbates on the fixed bed and the possibility of lighter molecules displacement with heavier ones in the bottom of the fixed bed reactor (where the adsorbates enter the adsorbent bed) might be responsible for the higher heel shown by mass balance and TGA for the fixed bed configuration. Further experiments were completed about competitive adsorption and the homogeneity of heel formation discussed in section 4.3 and 4.4.

4.2.2 Micropore – mesopore analysis

Since BAC is a primarily microporous material, adsorption takes place in micropores. Thus, the pore size distribution of the regenerated BAC samples from partial and full loading tests using the VOC mixture were investigated. Figure 4-7 shows the volume of micropores available for the regenerated BAC samples.

The specific surface area, total pore volume, and micropore volume (summarized in Table 4-2) decreased with adsorption and desorption processes compared to virgin BAC, which is attributed to irreversible adsorption on the adsorbent and pore blockage from bulky molecules such as naphthalene (Jahandar Lashaki et al., 2012b; Jahandar Lashaki et al., 2013). Molecules larger than the micropores can block the entrance to the pores and prevent nitrogen penetration and adsorption during micropore analysis. Moreover, these bulky molecules with high boiling points can displace lighter molecules from the narrow pores.

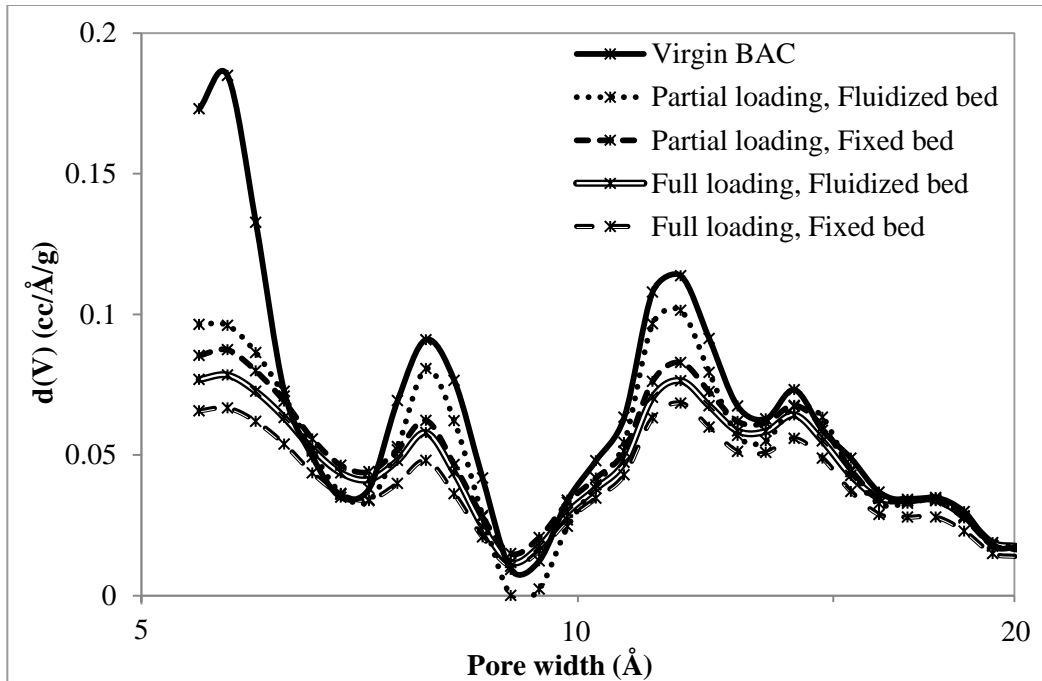


Figure 4-7 Effect of adsorbent bed configuration on pore size distribution of the regenerated BACs previously loaded with VOCs' mixture after five cycles

Table 4-2 Characterization summary for 5th cycle regenerated BAC samples loaded previously with VOC mixture

BAC sample	Surface area (m ² /g)	Total pore volume (cm ³ /g)	Micropore volume (cm ³ /g)
Virgin BAC	1349	0.57	0.47
Full loading, Fixed bed	897	0.38	0.32
Full loading, Fluidized bed	1045	0.45	0.37
Partial loading, Fixed bed	1116	0.47	0.38
Partial loading, Fluidized bed	1135	0.47	0.41

The available volume of micropores, especially narrow micropores, was higher for samples loaded in the fluidized bed configuration than in the fixed bed configuration, for both partially and fully loaded samples.

This difference in micropore loading between fixed bed and fluidized bed adsorption should be entirely attributed to differences during adsorption, because desorption occurred under identical conditions for both configurations (Figure 4-5 and Table 4-1). It is assumed that contact between adsorbent and adsorbate in the bottom part of the fixed BAC bed (where the adsorbate enters the reactor) and non – uniformity of adsorbates distribution is the reason for the higher occupancy and diffusion of adsorbate molecules into narrow micropores. This will make desorption more difficult in the bottom part of the fixed bed reactor. Furthermore, beads in the bottom part of the fixed bed reactor are saturated sooner than beads in the top of the reactor, which results in more displacement of the lighter compounds by the heavier ones in this part. For this reason TGA experiments were done for samples obtained from the top, middle, and bottom of the reactors, as explained in the next section.

4.3 Homogeneity of the adsorption – desorption bed

Because fluidization provides better mass transfer between the gas phase and the adsorbent, it was expected that the distribution of adsorbates on the BAC would be more uniform in the fluidized bed than in the fixed bed (Yazbek et al., 2006). For this reason, TGA was completed on regenerated BACs from the top, middle, and bottom of the fixed and fluidized bed reactors that were previously loaded with either 1,2,4 – trimethylbenzene or the VOC mixture during one cycle. The results are provided in Figure 4-8.

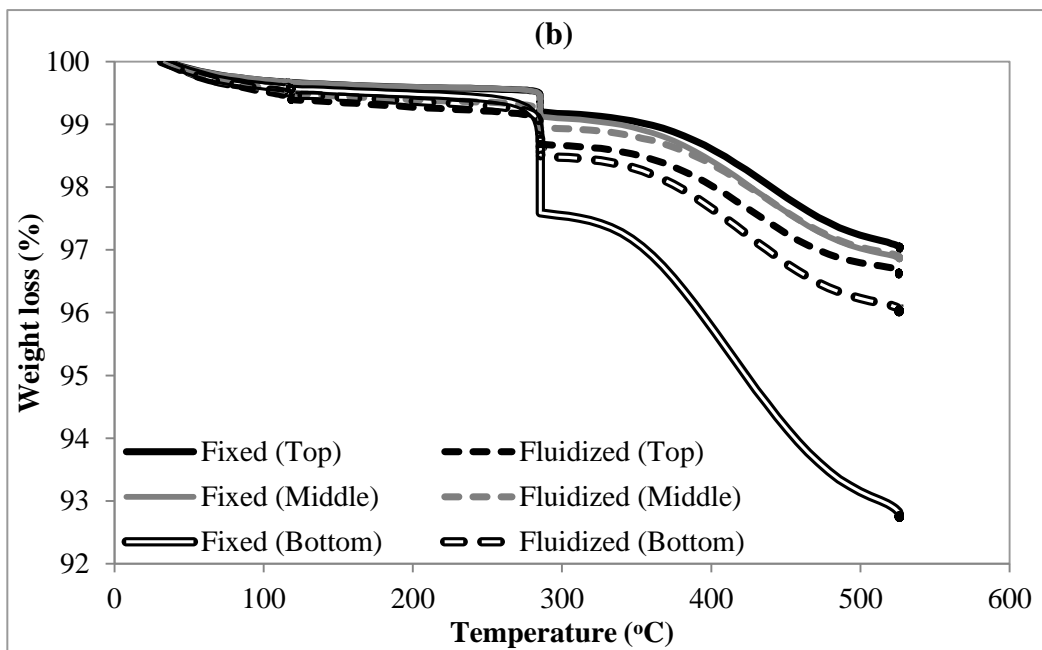
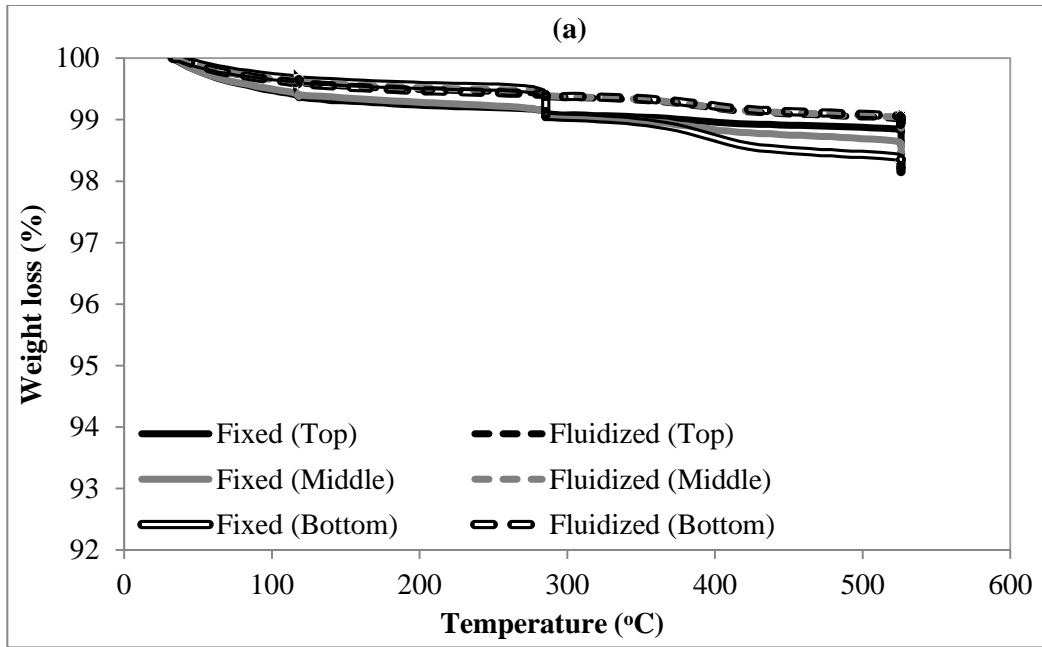


Figure 4-8 TGA results for regenerated BAC after one cycle adsorption from top, middle, and bottom of the reactors (a) 1,2,4 – trimethylbenzene and (b) VOC mixture

Comparing the weight change in the samples collected from the top, middle, and bottom of the reactor (Figure 4-8), non – uniform adsorbate distribution occurred in the fixed bed configuration while more uniform

distribution was found for the fluidized bed. This difference was more obvious for adsorption of the VOC mixture (Figure 4-8 (b)) which is attributed to the accumulation of heavier compounds in the bottom part of the reactor because of competitive adsorption in the fixed bed configuration. The TGA weight loss for the BAC in the bottom part of the fixed bed reactor was 3.0% while it was 7.3% for the top part.

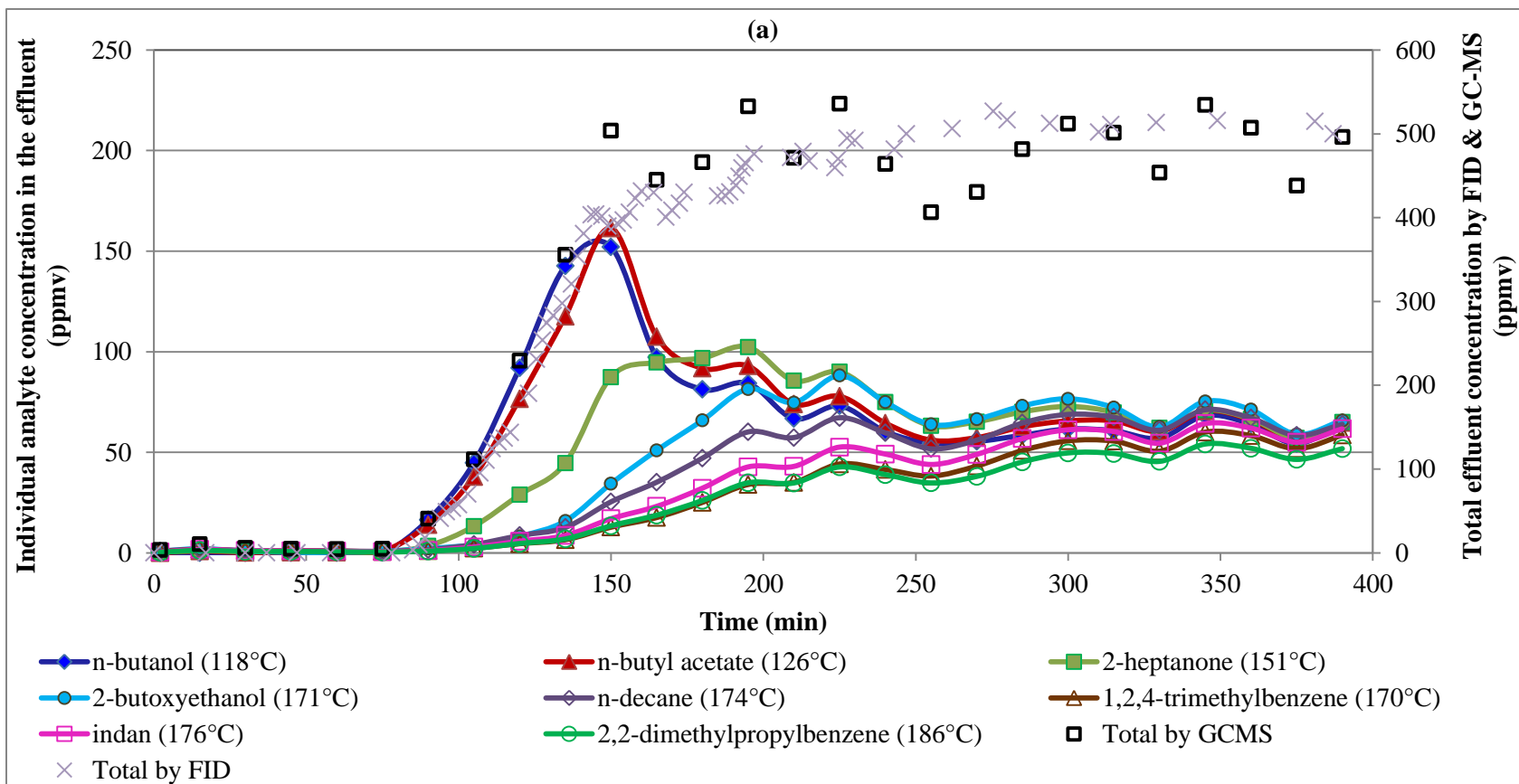
Hamed (2005) also showed uniform adsorbate (humidity) distribution on adsorbent (silica gel) in fluidized bed by detecting the color changes of silica gel during adsorption and found homogeneity in fluidized bed. They concluded the opposite in the fixed bed configuration that the adsorbate concentration adsorbed, decreased with the distance from the bottom of the fixed bed reactor, where the adsorbate stream enters (Hamed et al., 2010).

According to the above mentioned studies, a fixed bed configuration may inhibit proper contact between the adsorbate stream and the entire volume of adsorbent. When an adsorbate stream enters the fixed bed reactor, it first contacts a limited volume of adsorbent. For this reason the adsorbed compounds in the bottom parts of the fixed bed reactor are more likely to be replaced by heavier and bulkier molecules. In fluidized bed, however, the possibility for contacting adsorbates with unloaded adsorbent, which has high affinity for the VOC adsorption, is higher because of complete circulation of the adsorbent beads in the reactor. Therefore, the possibility of displacement of a light molecule by a heavier one is higher in the bottom part of the fixed bed, which results in higher pore blockage and increased presence of large molecules. The amount of these heavy molecules increases along the length of the fixed bed reactor during adsorption in the following cycles which leads to the higher heel formation in this configuration than in fluidized bed in the same adsorption time for both configurations.

4.4 Gas chromatography – mass spectrometry (GC – MS)

GC – MS experiments were completed using the reactors' effluent stream during adsorption of the modified VOC mixture containing eight organic

compounds (described in the methods section). The adsorption experiments were performed for 390 minutes in full loading of the BACs to compare the competitive adsorption in both fixed and fluidized bed configurations. Figure 4-9 shows the effluent concentration by FID and GC – MS for both fixed bed and fluidized bed adsorption. Breakthrough started (at effluent concentration of 1% of the inlet concentration) after 85 min and 97 min for fixed bed and fluidized bed configurations, respectively.



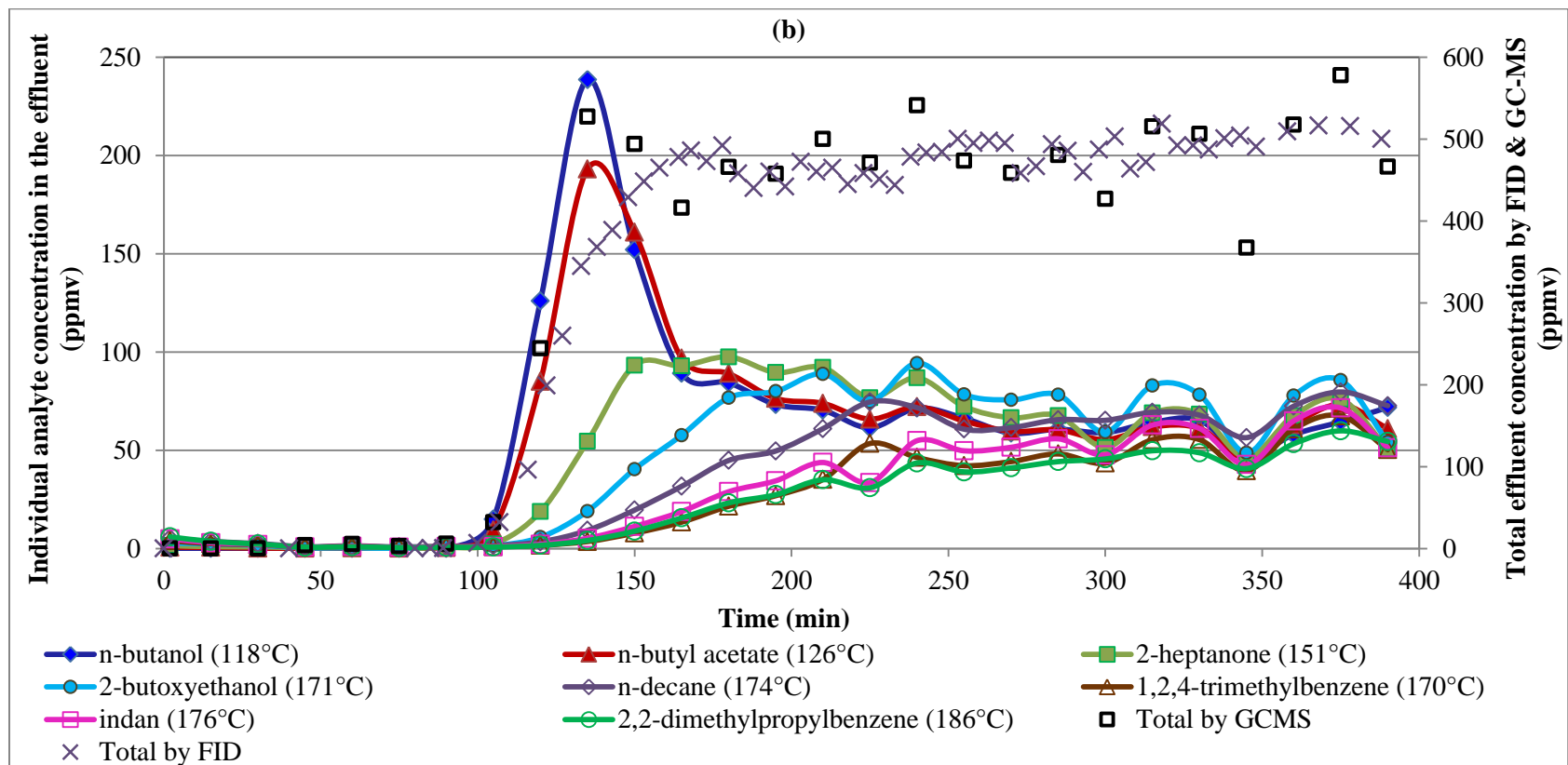


Figure 4-9 Effluent concentration during adsorption of modified VOC mixture on BAC in order of the components' retention time in GC (The boiling points are shown by the components in the legends) using (a) fixed bed and (b) fluidized bed configuration. The second axis on the right demonstrates the total adsorbates concentration measured by GC – MS and FID in the effluent.

n – butanol (118 °C) and n – butyl acetate (126 °C) were the first compounds detected by GC – MS. This represents the weak interaction between low boiling point compounds and carbon surface, and they can be displaced by higher boiling point components due to competitive adsorption (Lillo-Ródenas et al., 2006; Wang et al., 2012). The peaks in the concentration profiles of these low boiling point species are higher than their inlet concentrations due to the competitive adsorption and substitution of lighter compounds with heavier ones (Kim et al., 2001). The breakthrough curve is sharper for the fluidized bed, which is indicative of a shorter mass transfer zone (Carratalá-Abril et al., 2009).

Although breakthrough starts later in the fluidized bed, the lighter compounds' peaks appeared sooner and is higher than in the fixed bed. This can be better seen in Figure 4-10, which highlights initial VOC breakthrough for those tests described above. This shows faster and more facile displacement of the lighter compounds with the heavier ones for the fluidized bed configuration and might be attributed to better mass transfer between the gas and solid phases because of mixing during fluidization. While the shallower slope of the breakthrough curve in the fixed bed case can be attributed to non – uniformity of adsorption in the fixed bed resulting in re – adsorption of lighter molecules in the upper parts of the reactor.

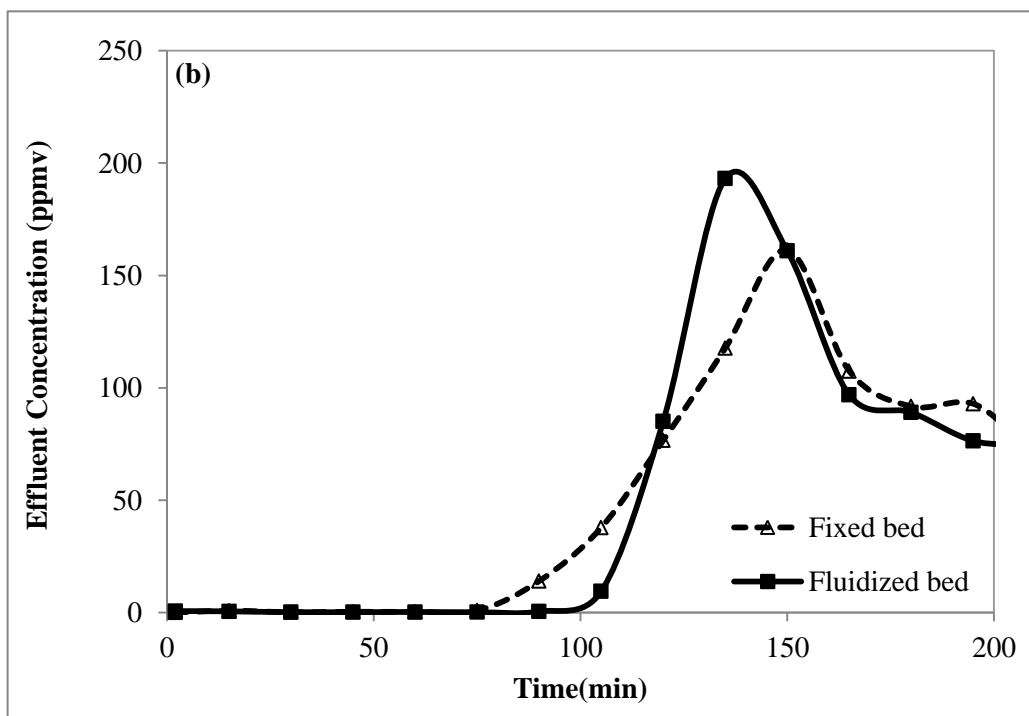
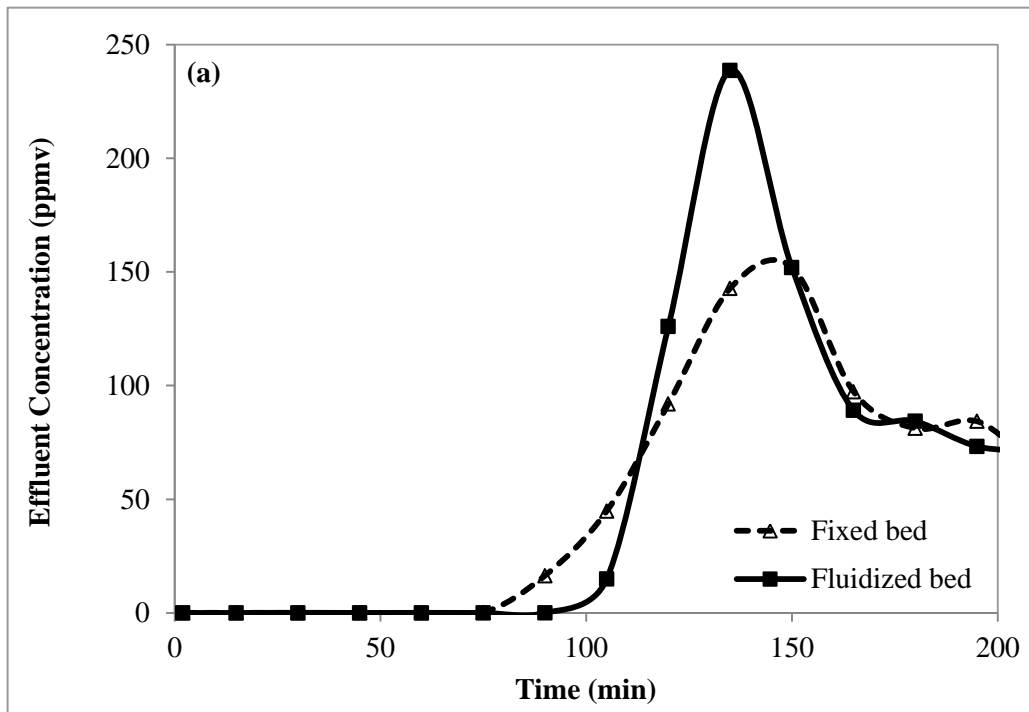
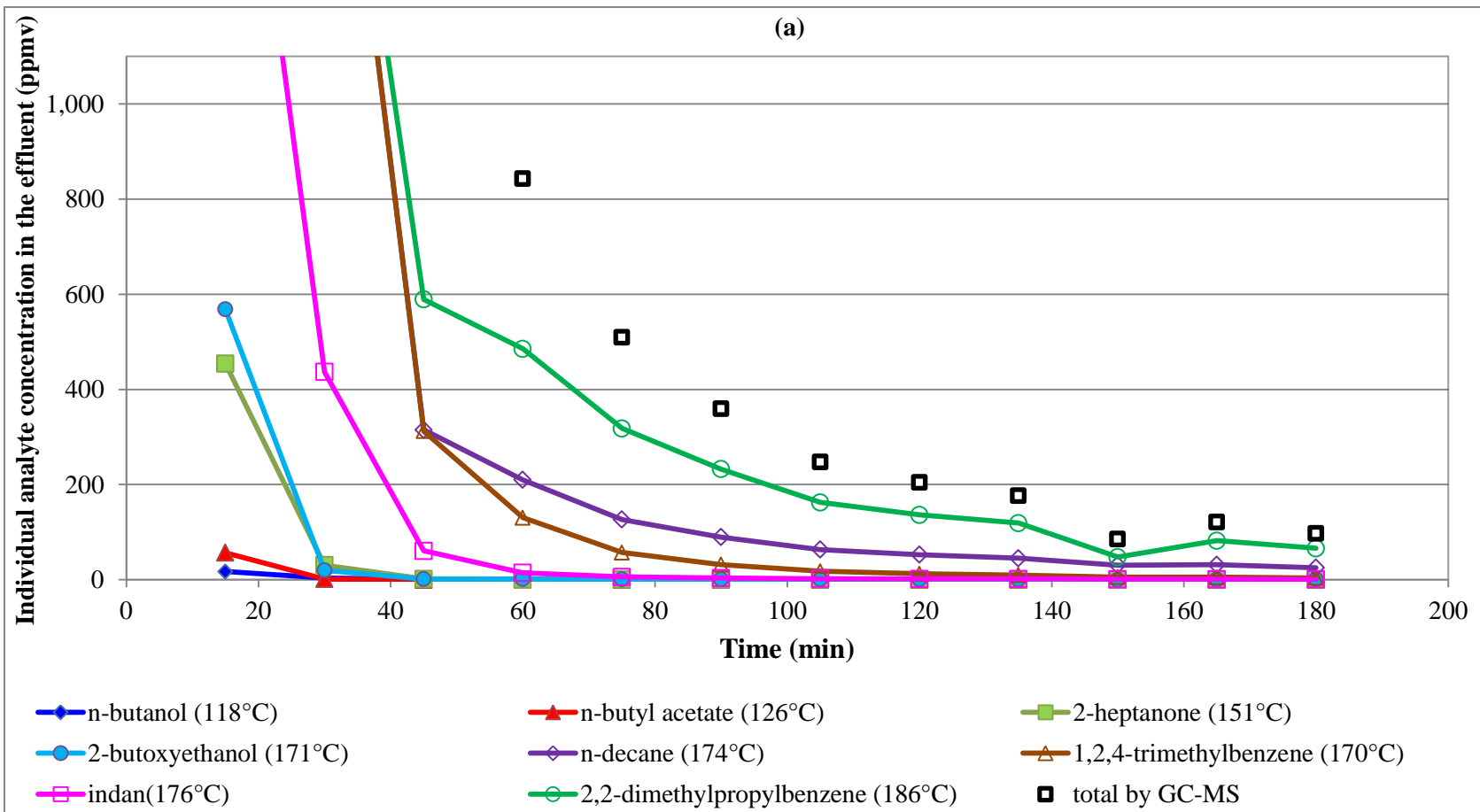


Figure 4-10 Effluent concentration of (a) n – butanol and (b) n – butyl acetate during adsorption on BAC using GC-MS

The concentration of the VOC components in the effluent stream (in order of increasing breakthrough time) were n – butanol (118 °C), n – butyl acetate (126 °C), 2 – heptanone (151 °C), 2 – butoxyethanol (171 °C), n – decane (174 °C), 1,2,4 – trimethylbenzene (170 °C), indan (176 °C), and 2,2 – dimethylpropylbenzene (186°C) in both configurations. Increasing the boiling point of the VOC component corresponds to increased breakthrough times, except for 1,2,4 – trimethylbenzene (O'Connor and Mueller, 2001; Wang et al., 2012). The longer breakthrough of this compound compared to 2 – butoxyethanol and n – decane might be attributed to its bulky structure. An aromatic ring with three side chains is notably different than the straight chain structures of n – decane and 2 – butoxyethanol, and desorption of bulkier molecules from micropores is more difficult due to diffusion (Wang et al., 2012). Generally, it is concluded that compounds with high boiling points and high molecular weights have more affinity to be adsorbed. For components with similar boiling points, molecular structure and functionalities must be considered (Li et al., 2012; Wang et al., 2012).

After adsorbing the modified VOC mixture using fixed and fluidized bed configurations, the adsorbent was regenerated in at 288 °C for 3 h. The desorbed gas was analyzed using GC – MS to determine the identity and concentration of the desorbing compounds. These results are given in Figure 4-11.



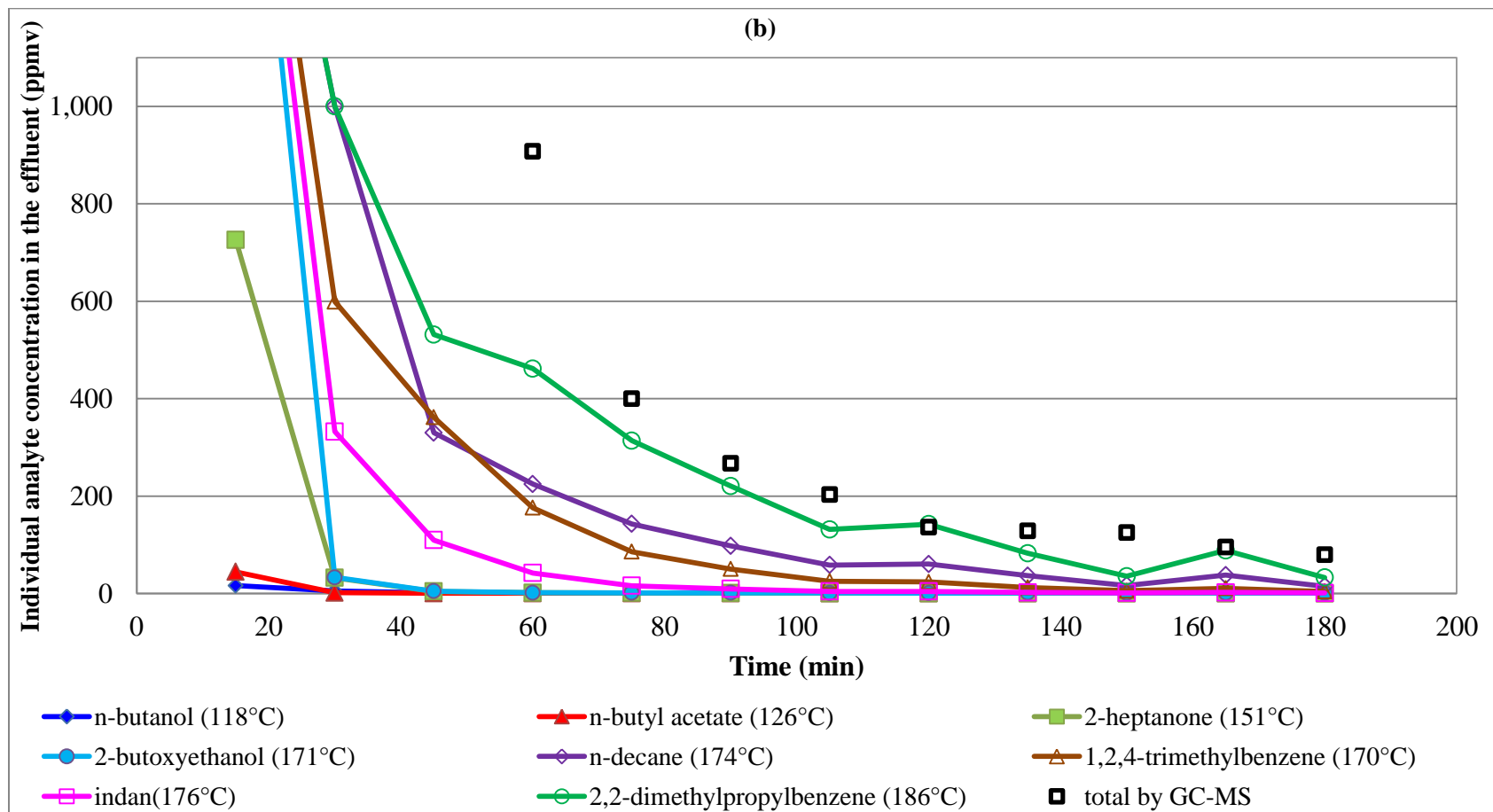


Figure 4-11 Concentrations of the organic species in the desorbing gas during regeneration of BAC previously saturated with modified VOC mixture using (a) fixed bed configuration and (b) fluidized bed configuration

Fewer light compounds were detected in the desorption stream, indicating that very low amount of these compounds remained on the BAC during adsorption. This supports the previous theory about displacement by heavier compounds. The concentration of the high boiling point components at the beginning of desorption was beyond the range of the GC – MS detector.

As time passed, the components' concentrations decreased and approached to zero. For lighter compounds, the concentrations reached zero before the heavier ones. 2,2 – dimethylpropylbenzene and n – decane were still detected after 3 h of thermal regeneration, which shows the higher energy requirements for desorption of high molecular weight compounds. Accumulation of bulky molecules with high molecular size, weight and boiling point, are responsible for inefficient thermal regeneration (Tanthapanichakoon et al., 2005).

Differences in the desorption of the BACs loaded in fixed bed and fluidized bed configurations include the detection of higher amount of 2-heptanone (151 °C) and 2-butoxyethanol (171 °C), which have moderate boiling point and molecular weight in comparison to other components of the mixture, in the effluent stream of the fluidized bed. This showed that competitive adsorption was less likely for these two compounds in fluidized bed than in the fixed bed configuration.

CHAPTER 5: CONCLUSION AND RECOMMENDATION

5.1 Conclusion

This research has added to the understanding of the effect of adsorption bed configuration on adsorption of volatile organic compounds (VOC) on beaded activated carbon (BAC) and its effect on irreversibility of adsorption. For this purpose, 1,2,4 – trimethylbenzene and a VOC mixture were used as a single component and multicomponent adsorbate stream. The adsorption experiments were completed in five consecutive cycles of partial and full loading of the adsorbent using both fixed and fluidized bed configuration in adsorption process with the same flow rate of air from below to the top of the reactors. All desorption tests were completed in fixed bed configuration for 3 hours in 288 °C with nitrogen gas flow as carrier gas followed by 50 minutes cooling. Also, supporting experiments were done using thermo – gravimetric analyzer (TGA), micropore analysis, and gas chromatography – mass spectrometry (GCMS). Important findings of this research were:

- Fluidized bed adsorption resulted in longer (13% for single component and 11% for VOC mixture) and sharper breakthrough profile than fixed bed configuration because of better mass transfer.
- Longer breakthrough time and sharper breakthrough profile in fluidized bed adsorption make this configuration more desirable for industry to obtain higher pollutants removal with zero emission.
- No discernible change was found in the adsorption capacity of the adsorbent using fixed and fluidized bed configurations either for single component or the mixture.
- Negligible (less than 1% by weight) heel formed in case of single component for both configurations consistent with the TGA results (1.2 –

1.6%) and the recovery of the adsorption capacity after each desorption step was apparent from close consecutive cycles breakthrough profiles

- The fluidized bed adsorption – fixed bed desorption showed 30 – 42% by weight lower heel formation after five consecutive cycles than fixed bed adsorption – fixed bed desorption cycles in full and partial loading. These results were also consistent with TGA results for both full and partial loading of the adsorbent (26 – 44% lower weight loss) and breakthrough curves for full loading experiments (38% lower breakthrough time reduction).

It can generally be concluded that the configuration can affect both adsorption kinetics and irreversible adsorption. Higher irreversible adsorption occurred for VOC mixture using fixed bed configuration that might be attributed to non – uniform adsorption in fixed bed. Since the heel formation was identical for all the experiments in case of single component and regarding to the TGA experiments completed on regenerated BAC samples from bottom, middle, and top of the reactor which previously been loaded with adsorbates, non – uniformity of the heel formation was observed in the fixed bed configuration in case of the mixture which might be attributed to the displacement of lighter compounds with heavier ones in the bottom part of the fixed bed reactor. The GC – MS results demonstrated shallow replacement of the lighter compounds with the heavier ones which is due to the re – adsorption of light molecules in top parts of the reactor.

5.2 Recommendations

Fluidized bed that is used for different applications in industry is better known for good mass transfer and low pressure drop. This research investigated fluidized bed configuration for adsorption processes in case of organic compounds and found higher adsorption kinetics and also lower irreversible adsorption beside the lower pressure drop obtained with this configuration comparing to fixed bed for a specific adsorbate mixture and adsorption – desorption system. Thus, more investigations are recommended to investigate the

effect of this configuration in adsorption for different mixtures. The findings might be different for other fluidization systems such as multistage fluidized bed or moving bed.

The other general recommendation is that the applicability of a laboratory scale in an industrial process always has to be checked with pilot scale systems since the small experimental, instrumental, and operator errors can cause larger errors in the results of the laboratory scale experiments than in pilot scale systems.

REFERENCES:

- Ahmad, A. A.; Idris, A. Preparation and characterization of activated carbons derived from bio-solid: A review. *Desalination and Water Treatment* **2013**, 51, 2554-2563.
- Ahmadpour, A.; Do, D. D. The preparation of active carbons from coal by chemical and physical activation. *Carbon* **1996**, 34, 471-479.
- Aktaş, Ö; Çeçen, F. Effect of type of carbon activation on adsorption and its reversibility. *Journal of Chemical Technology and Biotechnology* **2006**, 81, 94-101.
- Aktaş, Ö; Çeçen, F. Competitive adsorption and desorption of a bi-solute mixture: Effect of activated carbon type. *Adsorption* **2007**, 13, 159-169.
- Álvarez, P. M.; Beltrán, F. J.; Gómez-Serrano, V.; Jaramillo, J.; Rodríguez, E. M. Comparison between thermal and ozone regenerations of spent activated carbon exhausted with phenol. *Water Research* **2004**, 38, 2155-2165.
- Ania, C. O.; Menéndez, J. A.; Parra, J. B.; Pis, J. J. Microwave-induced regeneration of activated carbons polluted with phenol. A comparison with conventional thermal regeneration. *Carbon* **2004**, 42, 1377-1381.
- Ania, C. O.; Parra, J. B.; Menéndez, J. A.; Pis, J. J. Effect of microwave and conventional regeneration on the microporous and mesoporous network and on the adsorptive capacity of activated carbons. *Microporous and Mesoporous Materials* **2005**, 85, 7-15.
- Atkinson, R. Atmospheric chemistry of VOCs and NOx. *Atmospheric Environment* **2000**, 34, 2063-2101.
- Bansal, R. C.; Goyal, M. Activated carbon adsorption. Boca Raton: *Taylor & Francis*, **2005**.
- Benkhedda, J.; Jaubert, J. N.; Barth, D.; Perrin, L. Experimental and modeled results describing the adsorption of toluene onto activated carbon. *Journal of Chemical and Engineering Data* **2000**, 45, 650-653.
- Berenjian, A.; Chan, N.; Malmiri, H. J. Volatile Organic Compounds removal methods: A review. *American Journal of Biochemistry and Biotechnology* **2012**, 8, 220-229.
- Biron, E.; Evans, M. J. B. Dynamic adsorption of water-soluble and insoluble vapours on activated carbon. *Carbon* **1998**, 36, 1191-1197.
- Bottani, E. J.; Tascón, J. M. D. Adsorption by carbons. Amsterdam; London: *Elsevier*, **2008**.
- Bouhamra, W. S.; Baker, C. G. J.; Elkilani, A. S.; Alkandari, A. A.; Al-Mansour, A. A. Adsorption of toluene and 1,1,1-trichloroethane on selected adsorbents under a range of ambient conditions. *Adsorption* **2009**, 15, 461-475.
- Boulinguez, B.; Le Cloirec, P. Adsorption on activated carbons of five selected volatile organic compounds present in biogas: Comparison of granular and fiber cloth materials. *Energy and Fuels* **2010**, 24, 4756-4765.
- Bowman, F. M.; Seinfeld, J. H. Atmospheric chemistry of alternate fuels and reformulated gasoline components. *Progress in Energy and Combustion Science* **1995**, 21, 387-417.

- Broadhurst, T. E.; Becker, H. A. ONSET OF FLUIDIZATION AND SLUGGING IN BEDS OF UNIFORM PARTICLES. *AIChE Journal* **1975**, 21, 238-247.
- Brunauer, S.; Emmett, P. H.; Teller, E. Adsorption of gases in multimolecular layers. *Journal of the American Chemical Society* **1938**, 60, 309-319.
- Busca, G.; Berardinelli, S.; Resini, C.; Arrighi, L. Technologies for the removal of phenol from fluid streams: A short review of recent developments. *Journal of Hazardous Materials* **2008**, 160, 265-288.
- Carratalá-Abril, J.; Lillo-Ródenas, M. A.; Linares-Solano, A.; Cazorla-Amorós, D. Activated carbons for the removal of low-concentration gaseous toluene at the semipilot scale. *Industrial and Engineering Chemistry Research* **2009**, 48, 2066-2075.
- Cazorla-Amorós, D.; Alcaniz-Monge, J.; Linares-Solano, A. Characterization of activated carbon fibers by CO₂ adsorption. *Langmuir* **1996**, 12, 2820-2824.
- Chakma, A.; Meisen, A. Activated carbon adsorption of diethanolamine, methyl diethanolamine and their degradation products. *Carbon* **1989**, 27, 573-584.
- Cherbański, R.; Komorowska-Durka, M.; Stefanidis, G. D.; Stankiewicz, A. I. Microwave swing regeneration Vs temperature swing regeneration - Comparison of desorption kinetics. *Industrial and Engineering Chemistry Research* **2011**, 50, 8632-8644.
- Cherbański, R.; Molga, E. Intensification of desorption processes by use of microwaves-An overview of possible applications and industrial perspectives. *Chemical Engineering and Processing: Process Intensification* **2009**, 48, 48-58.
- Chiang, B. C.; Wey, M. Y.; Yang, W. Y. Control of incinerator organics by fluidized bed activated carbon adsorber. *Journal of Environmental Engineering* **2000**, 126, 985-992.
- Chiang, Y. C.; Chiang, P. C.; Huang, C. P. Effects of pore structure and temperature on VOC adsorption on activated carbon. *Carbon* **2001a**, 39, 523-534.
- Chiang, Y. C.; Chiang, P. E.; Chiang, P. C.; Chang, P. E.; Chang, E. E. Effects of surface characteristics of activated carbons on VOC adsorption. *Journal of Environmental Engineering* **2001b**, 127, 54-62.
- Chuang, C. L.; Chiang, P. C.; Chang, E. E. Kinetics of benzene adsorption onto activated carbon. *Environmental Science and Pollution Research* **2003a**, 10, 6-8.
- Chuang, C. L.; Chiang, P. C.; Chang, E. E.; Huang, C. P. Adsorption-desorption rate of nonpolar volatile organic compounds onto activated carbon exemplified by C₆H₆ and CCl₄. *Practice Periodical of Hazardous, Toxic, and Radioactive Waste Management* **2003b**, 7, 148-155.
- Cooper, C.D.; Alley, F.C. Air pollution control: A design approach (3rd ed.). Prospect Heights: *Waveland press*, **2002**.
- Dabek, L. Microwave regeneration of activated carbon. *Environment Protection Engineering* **2007**, 33, 107-115.

- Dąbrowski, A.; Podkościelny, P.; Hubicki, Z.; Barczak, M. Adsorption of phenolic compounds by activated carbon - A critical review. *Chemosphere* **2005**, 58, 1049-1070.
- Danielsson, M. A.; Hudon, V. VOC emission control using a fluidized-bed adsorption system. *Metal Finishing* **1994**, 92, 89-91.
- Das, D.; Gaur, V.; Verma, N. Removal of volatile organic compound by activated carbon fiber. *Carbon* **2004**, 42, 2949-2962.
- De Jonge, R. J.; Breure, A. M.; Van Andel, J. G. Reversibility of adsorption of aromatic compounds onto powdered activated carbon (PAC). *Water Research* **1996**, 30, 883-892.
- de Vasconcelos, P. D. S.; Mesquita, A. L. A. Minimum and full fluidization velocity for alumina used in the aluminum smelter. *International Journal of Engineering Business Management* **2011**, 3, 7-13.
- Delage, F.; Pre, P.; Le Cloirec, P. Mass transfer and warming during adsorption of high concentrations of VOCs on an activated carbon bed: Experimental and theoretical analysis. *Environmental Science and Technology* **2000**, 34, 4816-4821.
- Delage, F.; Pré, P.; Le Cloirec, P. Effects of moisture on warming of activated carbon bed during VOC adsorption. *Journal of Environmental Engineering* **1999**, 125, 1160-1167.
- Delebarre, A.; Morales, J. M.; Ramos, L. Influence of the bed mass on its fluidization characteristics. *Chemical Engineering Journal* **2004**, 98, 81-88.
- Díaz, E.; Ordóñez, S.; Vega, A.; Coca, J. Comparison of adsorption properties of a chemically activated and a steam-activated carbon, using inverse gas chromatography. *Microporous and Mesoporous Materials* **2005**, 82, 173-181.
- Dolidovich, A. F.; Akhremkova, G. S.; Efremtsev, V. S. Novel technologies of VOC decontamination in fixed, moving and fluidized catalyst-adsorbent beds. *Canadian Journal of Chemical Engineering* **1999**, 77, 342-355.
- Dombrowski, R. J.; Hyduke, D. R.; Lastoskie, C. M. Pore size analysis of activated carbons from argon and nitrogen porosimetry using density functional theory. *Langmuir* **2000**, 16, 5041-5050.
- U.S. Environmental Protection Agency. from <http://www.epa.gov>
- National Emission Inventory, Air Pollutant Emission Trends; U.S. Environmental Protection Agency. from <http://www.epa.gov/ttn/chieftrends/index.html>
- Fletcher, A. J.; Uygur, Y.; Thomas, M. K. Role of surface functional groups in the adsorption kinetics of water vapor on microporous activated carbons. *Journal of Physical Chemistry C* **2007**, 111, 8349-8359.
- Fletcher, A. J.; Yüzak, Y.; Thomas, K. M. Adsorption and desorption kinetics for hydrophilic and hydrophobic vapors on activated carbon. *Carbon* **2006**, 44, 989-1004.
- Franz, M.; Arafat, H. A.; Pinto, N. G. Effect of chemical surface heterogeneity on the adsorption mechanism of dissolved aromatics on activated carbon. *Carbon* **2000**, 38, 1807-1819.

- Geldart, D.; Rhodes, M. Developments in fluidisation. *Chemical Engineer (London)* **1986**, 30-32.
- Hamed, A. M. Theoretical and experimental study on the transient adsorption characteristics of a vertical packed porous bed. *Renewable Energy* **2002**, 27, 525-541.
- Hamed, A. M. Experimental investigation on the adsorption/desorption processes using solid desiccant in an inclined-fluidized bed. *Renewable Energy* **2005**, 30, 1913-1921.
- Hamed, A. M.; Abd El Rahman, W. R.; El-Eman, S. H. Experimental study of the transient adsorption/desorption characteristics of silica gel particles in fluidized bed. *Energy* **2010**, 35, 2468-2483.
- Harriott, P.; Cheng, A. T. Kinetics of spent activated carbon regeneration. *AIChE Journal* **1988**, 34, 1656-1662.
- Hashisho, Z.; Emamipour, H.; Rood, M. J.; Hay, K. J.; Kim, B. J.; Thurston, D. Concomitant adsorption and desorption of organic vapor in dry and humid air streams using microwave and direct electrothermal swing adsorption. *Environmental Science and Technology* **2008**, 42, 9317-9322.
- Hashisho, Z.; Rood, M.; Botich, L. Microwave-swing adsorption to capture and recover vapors from air streams with activated carbon fiber cloth. *Environmental Science and Technology* **2005**, 39, 6851-6859.
- Hashisho, Z.; Rood, M. J.; Barot, S.; Bernhard, J. Role of functional groups on the microwave attenuation and electric resistivity of activated carbon fiber cloth. *Carbon* **2009**, 47, 1814-1823.
- Huang, M. C.; Chou, C. H.; Teng, H. Pore-size effects on activated-carbon capacities for volatile organic compound adsorption. *AIChE Journal* **2002**, 48, 1804-1810.
- Huang, Z. H.; Kang, F.; Liang, K. M.; Hao, J. Breakthrough of methylethylketone and benzene vapors in activated carbon fiber beds. *Journal of Hazardous Materials* **2003**, 98, 107-115.
- Hung, H. W.; Lin, T. F. Prediction of the adsorption capacity for volatile organic compounds onto activated carbons by the Dubinin-Radushkevich-Langmuir model. *Journal of the Air and Waste Management Association* **2007**, 57, 497-506.
- Jahandar Lashaki, M.; Fayaz, M.; Niknaddaf, S.; Hashisho, Z. Effect of the adsorbate kinetic diameter on the accuracy of the Dubinin-Radushkevich equation for modeling adsorption of organic vapors on activated carbon. *Journal of Hazardous Materials* **2012a**, 241-242, 154-163.
- Jahandar Lashaki, M.; Fayaz, M.; Wang, H.; Hashisho, Z.; Philips, J. H.; Anderson, J. E.; Nichols, M. Effect of adsorption and regeneration temperature on irreversible adsorption of organic vapors on beaded activated carbon. *Environmental Science and Technology* **2012b**, 46, 4083-4090.
- Jahandar Lashaki, M.; Shariaty, P.; S., Kamravaei; Fayaz, M.; Hashisho, Z. Effect of adsorption carrier gas on the irreversible adsorption of a mixture of organic vapors. *In the proceedings of 106th annual Air and Waste Management Association (AWMA) conference exhibition* **2013**.

- Kampa, M.; Castanas, E. Human health effects of air pollution. *Environmental Pollution* **2008**, 151, 362-367.
- Kaneko, Y.; Ohbu, K.; Uekawa, N.; Fujie, K.; Kaneko, K. Evaluation of low concentrated hydrophilic sites on microporous carbon surfaces with an X-ray photoelectron spectroscopy ratio method. *Langmuir* **1995**, 11, 708-710.
- Kawasaki, N.; Kinoshita, H.; Oue, T.; Nakamura, T.; Tanada, S. Study on adsorption kinetic of aromatic hydrocarbons onto activated carbon in gaseous flow method. *Journal of Colloid and Interface Science* **2004**, 275, 40-43.
- Khan, F. I.; Ghoshal, Kr. A. Removal of Volatile Organic Compounds from polluted air. *Journal of Loss Prevention in the Process Industries* **2000**, 13, 527-545.
- Kim, B. R. VOC emissions from automotive painting and their control: A review. *Environmental Engineering Research* **2011**, 16, 1-9.
- Kim, B. R.; Podsiadlik, D. H.; Yeh, D. H.; Salmeen, I. T.; Briggs, L. M. Evaluating the conversion of an automotive paint spray-booth scrubber to an activated-sludge system for removing paint volatile organic compounds from air. *Water Environment Research* **1997**, 69, 1211-1221.
- Kim, J. H.; Ryu, Y. K.; Haam, S.; Lee, C. H.; Kim, W. S. Adsorption and steam regeneration of n-hexane, MEK, and toluene on activated carbon fiber. *Separation Science and Technology* **2001**, 36, 263-281.
- Kunii, D.; Levenspiel, O. Fluidization engineering. New York: *Wiley*, **1969**.
- Langmuir, I. The adsorption of gases on plane surfaces of glass, mica and platinum. *The Journal of the American Chemical Society* **1918**, 40, 1361-1403.
- Lapkin, A.; Joyce, L.; Crittenden, B. Framework for evaluating the "greenness" of chemical processes: Case studies for a novel VOC recovery technology. *Environmental Science and Technology* **2004**, 38, 5815-5823.
- Lee, M. G.; Lee, S. W.; Lee, S. H. Comparison of vapor adsorption characteristics of acetone and toluene based on polarity in activated carbon fixed-bed reactor. *Korean Journal of Chemical Engineering* **2006**, 23, 773-778.
- Leslie, G. B. Health risks from indoor air pollutants: Public alarm and toxicological reality. *Indoor and Built Environment* **2000**, 9, 5-16.
- Li, L.; Liu, S.; Liu, J. Surface modification of coconut shell based activated carbon for the improvement of hydrophobic VOC removal. *Journal of Hazardous Materials* **2011**, 192, 683-690.
- Li, L.; Sun, Z.; Li, H.; Keener, T. C. Effects of activated carbon surface properties on the adsorption of volatile organic compounds. *Journal of the Air and Waste Management Association* **2012**, 62, 1196-1202.
- Lillo-Ródenas, M. A.; Cazorla-Amorós, D.; Linares-Solano, A. Behaviour of activated carbons with different pore size distributions and surface oxygen groups for benzene and toluene adsorption at low concentrations. *Carbon* **2005**, 43, 1758-1767.

- Lillo-Ródenas, M. A.; Cazorla-Amorós, D.; Linares-Solano, A. Benzene and toluene adsorption at low concentration on activated carbon fibres. *Adsorption* **2011**, *17*, 473-481.
- Lillo-Ródenas, M. A.; Fletcher, A. J.; Thomas, K. M.; Cazorla-Amorós, D.; Linares-Solano, A. Competitive adsorption of a benzene-toluene mixture on activated carbons at low concentration. *Carbon* **2006**, *44*, 1455-1463.
- Lin, C. L.; Cheng, Y. H.; Liu, Z. S.; Chen, J. Y. Adsorption and oxidation of high concentration toluene with activated carbon fibers. *Journal of Porous Materials* **2013**, *20*, 883-889.
- Lippens, B. C.; de Boer, J. H. Studies on pore systems in catalysts. V. The t method. *Journal of Catalysis* **1965**, *4*, 319-323.
- Liu, P. K. T.; Feltch, S. M.; Wagner, N. J. Thermal desorption behavior of aliphatic and aromatic hydrocarbons loaded on activated carbon. *Industrial and Engineering Chemistry Research* **1987**, *26*, 1540-1545.
- Lu, Q.; Sorial, G. A. The role of adsorbent pore size distribution in multicomponent adsorption on activated carbon. *Carbon* **2004**, *42*, 3133-3142.
- Lu, Q.; Sorial, G. A. A comparative study of multicomponent adsorption of phenolic compounds on GAC and ACFs. *Journal of Hazardous Materials* **2009**, *167*, 89-96.
- Mahajan, O. P.; Moreno-Castilla, C.; Walker Jr, P. L. Surface-treated activated carbon for removal of phenol from water. *Separation Science and Technology* **1980**, *15*, 1733-1752.
- Maroto-Valer, M. M.; Dranca, I.; Clifford, D.; Lupascu, T.; Nastas, R.; Leon y Leon, C. A. Thermal regeneration of activated carbons saturated with ortho- and meta-chlorophenols. *Thermochimica Acta* **2006**, *444*, 148-156.
- McEnaney, B. Adsorption and structure in microporous carbons. *Carbon* **1988**, *26*, 267-274.
- Mikhail, R. S.; Brunauer, S.; Bodor, E. E. Investigations of a complete pore structure analysis. I. Analysis of micropores. *Journal of Colloid And Interface Science* **1968**, *26*, 45-53.
- Mohan, N.; Kannan, G. K.; Upendra, S.; Subha, R.; Kumar, N. S. Breakthrough of toluene vapours in granular activated carbon filled packed bed reactor. *Journal of Hazardous Materials* **2009**, *168*, 777-781.
- Mohanty, C. R.; Meikap, B. C. Pressure drop characteristics of a multi-stage counter-current fluidized bed reactor for control of gaseous pollutants. *Chemical Engineering and Processing: Process Intensification* **2009**, *48*, 209-216.
- Nastaj, J. F.; Ambrozek, B.; Rudnicka, J. Simulation studies of a vacuum and temperature swing adsorption process for the removal of VOC from waste air streams. *International Communications in Heat and Mass Transfer* **2006**, *33*, 80-86.
- Ng, Y. L.; Yan, R.; Tsen, L. T. S.; Yong, L. C.; Liu, M.; Liang, D. T. Volatile organic compound adsorption in a gas-solid fluidized bed. *Water Science and Technology* **2004**, *50*, 233-240.

- O'Connor, T. P.; Mueller, J. Modeling competitive adsorption of chlorinated volatile organic compounds with the Dubinin-Radushkevich equation. *Microporous and Mesoporous Materials* **2001**, 46, 341-349.
- Olivier, J. P. Improving the models used for calculating the size distribution of micropore volume of activated carbons from adsorption data. *Carbon* **1998**, 36, 1469-1472.
- Pabiś, A.; Magiera, J. Measurements of porosity of a gas-solid fluidized bed. *Advanced Powder Technology* **2002**, 13, 347-362.
- Pariselli, F.; Sacco, M. G.; Ponti, J.; Rembges, D. Effects of toluene and benzene air mixtures on human lung cells (A549). *Experimental and Toxicologic Pathology* **2009**, 61, 381-386.
- Parmar, G. R.; Rao, N. N. Emerging control technologies for volatile organic compounds. *Critical Reviews in Environmental Science and Technology* **2009**, 39, 41-78.
- Pei, J.; Zhang, J. S. Determination of adsorption isotherm and diffusion coefficient of toluene on activated carbon at low concentrations. *Building and Environment* **2012**, 48, 66-76.
- Pesaran, A. A.; Mills, A. F. Moisture transport in silica gel packed beds- I. Theoretical study. *International Journal of Heat and Mass Transfer* **1987**, 30, 1037-1049.
- Pires, J.; Pinto, M.; Carvalho, A.; Brotas de Carvalho, M. Adsorption of acetone, methyl ethyl ketone, 1,1,1-trichloroethane, and trichloroethylene in granular activated carbons. *Journal of Chemical and Engineering Data* **2003**, 48, 416-420.
- Popescu, M.; Joly, J. P.; Carré, J.; Danatou, C. Dynamical adsorption and temperature-programmed desorption of VOCs (toluene, butyl acetate and butanol) on activated carbons. *Carbon* **2003**, 41, 739-748.
- Ramalingam, S. G.; Pré, P.; Giraudet, S.; Le Coq, L.; Le Cloirec, P.; Baudouin, O.; Déchelotte, S. Different families of volatile organic compounds pollution control by microporous carbons in temperature swing adsorption processes. *Journal of Hazardous Materials* **2012**, 221-222, 242-247.
- Ramírez, N.; Cuadras, A.; Rovira, E.; Borrull, F.; Marcé, R. M. Comparative study of solvent extraction and thermal desorption methods for determining a wide range of volatile organic compounds in ambient air. *Talanta* **2010**, 82, 719-727.
- Ravikovitch, P. I.; Neimark, A. V. Density functional theory model of adsorption on amorphous and microporous silica materials. *Langmuir* **2006**, 22, 11171-11179.
- Reichhold, A.; Hofbauer, H. Internally circulating fluidized bed for continuous adsorption and desorption. *Chemical Engineering and Processing: Process Intensification* **1995**, 34, 521-527.
- Reuß, J.; Bathen, D.; Schmidt-Traub, H. Desorption by microwaves: Mechanisms of multicomponent mixtures. *Chemical Engineering and Technology* **2002**, 25, 381-384.
- Rivera-Utrilla, J.; Ferro-García, M. A.; Bautista-Toledo, I.; Sánchez-Jiménez, C.; Salvador, F.; Merchán, M. D. Regeneration of ortho-chlorophenol-

- exhausted activated carbons with liquid water at high pressure and temperature. *Water Research* **2003**, 37, 1905-1911.
- Romero-Anaya, A. J.; Lillo-Ródenas, M. A.; Linares-Solano, A. Spherical activated carbons for low concentration toluene adsorption. *Carbon* **2010**, 48, 2625-2633.
- Roy, S.; Mohanty, C. R.; Meikap, B. C. Multistage fluidized bed reactor performance characterization for adsorption of carbon dioxide. *Industrial and Engineering Chemistry Research* **2009**, 48, 10718-10727.
- Rudling, J.; Björkholm, E. Irreversibility effects in liquid desorption of organic solvents from activated carbon. *Journal of Chromatography A* **1987**, 392, 239-248.
- Ruhl, J. Reducing the pressures of VOC recovery. *Pollution Engineering* **2000**, 32, 40-43.
- Sabio, E.; González, E.; González, J. F.; González-García, C. M.; Ramiro, A.; Gañan, J. Thermal regeneration of activated carbon saturated with p-nitrophenol. *Carbon* **2004**, 42, 2285-2293.
- Salvador, F.; Jiménez, C. S. A new method for regenerating activated carbon by thermal desorption with liquid water under subcritical conditions. *Carbon* **1996**, 34, 511-516.
- San Miguel, G.; Lambert, S. D.; Graham, N. J. D. The regeneration of field-spent granular-activated carbons. *Water Research* **2001**, 35, 2740-2748.
- Sanders, R. E. Designs that lacked inherent safety: Case histories. *Journal of Hazardous Materials* **2003**, 104, 149-161.
- Saxena, S. C.; Vadivel, R. Wall effects in gas-fluidized beds at incipient fluidization. *Chemical Engineering Journal* **1988**, 39, 133-137.
- Scholz, M.; Martin, R. J. Control of bio-regenerated granular activated carbon by spreadsheet modelling. *Journal of Chemical Technology and Biotechnology* **1998**, 71, 253-261.
- Schweiger, T. A. J.; LeVan, M. D. Steam regeneration of solvent adsorbers. *Industrial and Engineering Chemistry Research* **1993**, 32, 2418-2429.
- Sheintuch, M.; Matatov-Meytal, Y. I. Comparison of catalytic processes with other regeneration methods of activated carbon. *Catalysis Today* **1999**, 53, 73-80.
- Shonnard, D. R.; Hiew, D. S. Comparative environmental assessment of VOC recovery and recycle design alternatives for a gaseous waste stream. *Environmental Science and Technology* **2000**, 34, 5222-5228.
- Silvestre-Albero, A.; Ramos-Fernández, J. M.; Martínez-Escandell, M.; Sepúlveda-Escribano, A.; Silvestre-Albero, J.; Rodríguez-Reinoso, F. High saturation capacity of activated carbons prepared from mesophase pitch in the removal of volatile organic compounds. *Carbon* **2010**, 48, 548-556.
- Singh, K. P.; Mohan, D.; Tandon, G. S.; Gupta, G. S. D. Vapor-phase adsorption of hexane and benzene on activated carbon fabric cloth: Equilibria and rate studies. *Industrial and Engineering Chemistry Research* **2002**, 41, 2480-2486.

- Song, W.; Tondeur, D.; Luo, L.; Li, J. VOC adsorption in circulating gas fluidized bed. *Adsorption* **2005**, 11, 853-858.
- Stein, M.; Ding, Y. L.; Seville, J. P. K.; Parker, D. J. Solids motion in bubbling gas fluidized beds. *Chemical Engineering Science* **2000**, 55, 5291-5300.
- Su, C. H.; Wu, S. H.; Shen, S. J.; Shiue, G. Y.; Wang, Y. W.; Shu, C. M. Thermal characteristics and regeneration analyses of adsorbents by differential scanning calorimetry and scanning electron microscope. *Journal of Thermal Analysis and Calorimetry* **2009**, 96, 765-769.
- Sullivan, P. D.; Rood, M. J.; Dombrowski, K. D.; Hay, K. J. Capture of organic vapors using adsorption and electrothermal regeneration. *Journal of Environmental Engineering* **2004**, 130, 258-267.
- Sullivan, P. D.; Rood, M. J.; Hay, K. J.; Qi, S. Adsorption and electrothermal desorption of hazardous organic vapors. *Journal of Environmental Engineering* **2001**, 127, 217-223.
- Sullivan, P. D.; Stone, B. R.; Hashisho, Z.; Rood, M. J. Water adsorption with hysteresis effect onto microporous activated carbon fabrics. *Adsorption* **2007**, 13, 173-189.
- Suzuki, M. Adsorption engineering. Amsterdam ; New York: *Elsevier*, **1990**.
- Suzuki, M.; Misic, D. M.; Koyama, O.; Kawazoe, K. Study of thermal regeneration of spent activated carbons: Thermogravimetric measurement of various single component organics loaded on activated carbons. *Chemical Engineering Science* **1978**, 33, 271-279.
- Tamon, H.; Okazaki, M. Desorption characteristics of aromatic compounds in aqueous solution on solid adsorbents. *Journal of Colloid and Interface Science* **1996**, 179, 181-187.
- Tancrede, M.; Wilson, R.; Zeise, L.; Crouch, E. A. C. The carcinogenic risk of some organic vapors indoors: A theoretical survey. *Atmospheric Environment* **1987**, 21, 2187-2205.
- Tanthapanichakoon, W.; Ariyadejwanich, P.; Japthong, P.; Nakagawa, K.; Mukai, S. R.; Tamon, H. Adsorption-desorption characteristics of phenol and reactive dyes from aqueous solution on mesoporous activated carbon prepared from waste tires. *Water Research* **2005**, 39, 1347-1353.
- Tsai, J. H.; Chiang, H. M.; Huang, G. Y.; Chiang, H. L. Adsorption characteristics of acetone, chloroform and acetonitrile on sludge-derived adsorbent, commercial granular activated carbon and activated carbon fibers. *Journal of Hazardous Materials* **2008**, 154, 1183-1191.
- Van Deventer, J. S. J.; Camby, B. S. Kinetics of the thermal regeneration of spent activated carbon in a fluidized bed. *Thermochimica Acta* **1988**, 136, 179-189.
- Varma, Y. B. G. Pressure drop of the fluid and the flow patterns of the phases in multistage fluidisation. *Powder Technology* **1975**, 12, 167-174.
- Villacañas, F.; Pereira, M. F. R.; Órfão, J. J. M.; Figueiredo, J. L. Adsorption of simple aromatic compounds on activated carbons. *Journal of Colloid and Interface Science* **2006**, 293, 128-136.
- Wang, H.; Jahandar Lashaki, M.; Fayaz, M.; Hashisho, Z.; Philips, J. H.; Anderson, J. E.; Nichols, M. Adsorption and desorption of mixtures of

- organic vapors on beaded activated carbon. *Environmental Science and Technology* **2012**, 46, 8341-8350.
- Wang, J.; Kaskel, S. KOH activation of carbon-based materials for energy storage. *Journal of Materials Chemistry* **2012**, 22, 23710-23725.
- Wang, L.; Balasubramanian, N. Electrochemical regeneration of granular activated carbon saturated with organic compounds. *Chemical Engineering Journal* **2009**, 155, 763-768.
- Wang, Q.; Liang, X. Y.; Zhang, R.; Liu, C. J.; Liu, X. J.; Qiao, W. M.; Zhan, L.; Ling, L. C. Preparation of polystyrene-based activated carbon spheres and their adsorption of dibenzothiophene. *Xinxing Tan Cailiao/ New Carbon Materials* **2009**, 24, 55-59.
- Wherrett, M. R.; Ryan, P. A. VOC emissions from industrial painting processes as a source of fuel cell energy. *Metal Finishing* **2004**, 102, 23-29.
- Xu, B. H.; Yu, A. B. Numerical simulation of the gas-solid flow in a fluidized bed by combining discrete particle method with computational fluid dynamics. *Chemical Engineering Science* **1997**, 52, 2785-2809.
- Yan, L.; Sorial, G. Novel tailored activated carbon for hampering surface oligomerization of organic compounds. *In the proceedings of 242nd American Chemical Society (ACS) National Meeting and Exposition* **2011**.
- Yang, J.; Zhao, Q.; Xu, H.; Li, L.; Dong, J.; Li, J. Adsorption of CO₂, CH₄, and N₂ on gas diameter grade ion-exchange small pore zeolites. *Journal of Chemical and Engineering Data* **2012**, 57, 3701-3709.
- Yang, R. T. Gas separation by adsorption processes. London: *Imperial college press*, **1997**.
- Yazbek, W.; Pré, P.; Delebarre, A. Adsorption and desorption of volatile organic compounds in fluidized bed. *Journal of Environmental Engineering* **2006**, 132, 442-452.
- Yenisoy-Karakaş, S.; Aygün, A.; Güneş, M.; Tahtasakal, E. Physical and chemical characteristics of polymer-based spherical activated carbon and its ability to adsorb organics. *Carbon* **2004**, 42, 477-484.
- Yonge, D. R.; Keinath, T. M.; Poznanska, K.; Jiang, Z. P. Single-solute irreversible adsorption on granular activated carbon. *Environmental Science and Technology* **1985**, 19, 690-694.

Appendix A: Mass balance for adsorption of 500 ppmv 1,2,4 – trimethylbenzene on virgin BAC

Table A - 1 Mass balance of 1,2,4 – trimethylbenzene adsorption on virgin BAC (Full loading, Fixed bed)

Test No.	Amount of virgin BAC (g)	Amount adsorbed (g)	% adsorption capacity (g adsorbed / g adsorbent)
1	6.98	3.17	45.51
2	6.99	3.20	45.79
3	6.99	3.19	45.71
4	7.00	3.16	45.18
5	7.03	3.12	44.46
6	6.96	3.19	45.82

Table A - 2 Mass balance of 1,2,4 – trimethylbenzene adsorption on virgin BAC (Full loading, Fluidized bed)

Test No.	Amount of virgin BAC (g)	Amount adsorbed (g)	% adsorption capacity (g adsorbed / g adsorbent)
1	7.01	3.20	45.68
2	7.00	3.22	46.02
3	7.00	3.07	43.89
4	7.01	3.21	45.82

Table A - 3 Mass balance of 1,2,4 – trimethylbenzene adsorption on virgin BAC (Partial loading, Fixed bed)

Test No.	Amount of virgin BAC (g)	Amount adsorbed (g)	% adsorption capacity (g adsorbed / g adsorbent)
1	7.01	2.15	30.71
2	7.01	2.12	30.28

Table A - 4 Mass balance of 1,2,4 – trimethylbenzene adsorption on virgin BAC (Partial loading, Fluidized bed)

Test No.	Amount of virgin BAC (g)	Amount adsorbed (g)	% adsorption capacity (g adsorbed / g adsorbent)
1	7.02	2.17	30.92
2	7.00	2.08	29.64

Appendix B: five cycles of Adsorption – desorption of 1,2,4 – trimethylbenzene on BAC

Table B - 1 Mass balance of 1,2,4 – trimethylbenzene adsorption – desorption on BAC (Full loading Fixed bed), 1st run

Weight Dry virgin BAC used: 7.03 g				
Cycle	Amount adsorbed (g)	% adsorption capacity (g adsorbed / g adsorbent)	Total heel formed (g)	% accumulated heel formation (g adsorbate remained / g adsorbent)
1	3.12	44.46	0.12	1.68
2	3.07	43.63	0.07	1.07
3	3.11	44.20	0.06	0.88
4	3.12	44.36	0.06	0.90
5	3.11	44.27	0.06	0.85

Table B - 2 Mass balance of 1,2,4 – trimethylbenzene adsorption – desorption on BAC (Full loading Fixed bed), 2nd run

Weight Dry virgin BAC used: 6.96 g				
Cycle	Amount adsorbed (g)	% adsorption capacity (g adsorbed / g adsorbent)	Total heel formed (g)	% accumulated heel formation (g adsorbate remained / g adsorbent)
1	3.19	45.82	0.02	0.36
2	3.15	45.24	0.04	0.55
3	3.12	44.90	0.01	0.12
4	3.16	45.49	0.03	0.39
5	3.14	45.11	0.04	0.55

Table B - 3 Mass balance of 1,2,4 – trimethylbenzene adsorption – desorption on BAC (Full loading Fluidized bed), 1st run

Weight Dry virgin BAC used: 7.00 g				
Cycle	Amount adsorbed (g)	% adsorption capacity (g adsorbed / g adsorbent)	Total heel formed (g)	% accumulated heel formation (g adsorbate remained / g adsorbent)
1	3.07	43.89	0.05	0.70
2	3.01	42.97	0.04	0.57
3	3.03	43.24	0.05	0.67
4	2.98	42.50	0.05	0.71
5	2.92	41.67	0.04	0.53

Table B - 4 Mass balance of 1,2,4 – trimethylbenzene adsorption – desorption on BAC (Full loading Fluidized bed), 2nd run

Weight Dry virgin BAC used: 7.01 g				
Cycle	Amount adsorbed (g)	% adsorption capacity (g adsorbed / g adsorbent)	Total heel formed (g)	% accumulated heel formation (g adsorbate remained / g adsorbent)
1	3.21	45.82	0.03	0.46
2	3.19	45.60	0.03	0.43
3	3.18	45.32	0.04	0.56
4	3.19	45.52	0.05	0.70
5	3.17	45.23	0.06	0.79

Table B - 5 Mass balance of 1,2,4 – trimethylbenzene adsorption – desorption on BAC (Partial loading Fixed bed), 1st run

Weight Dry virgin BAC used: 7.01 g				
Cycle	Amount adsorbed (g)	% adsorption capacity (g adsorbed / g adsorbent)	Total heel formed (g)	% accumulated heel formation (g adsorbate remained / g adsorbent)
1	2.15	30.71	0.04	0.51
2	2.20	31.44	0.04	0.54
3	2.16	30.82	0.05	0.67
4	2.15	30.71	0.05	0.64
5	2.17	31.01	0.05	0.70

Table B - 6 Mass balance of 1,2,4 – trimethylbenzene adsorption – desorption on BAC (Partial loading Fixed bed), 2nd run

Weight Dry virgin BAC used: 7.01 g				
Cycle	Amount adsorbed (g)	% adsorption capacity (g adsorbed / g adsorbent)	Total heel formed (g)	% accumulated heel formation (g adsorbate remained / g adsorbent)
1	2.12	30.28	0.03	0.44
2	2.15	30.75	0.02	0.30
3	2.15	30.75	0.01	0.11
4	2.16	30.83	0.02	0.30
5	2.18	31.12	0.03	0.46

Table B - 7 Mass balance of 1,2,4 – trimethylbenzene adsorption – desorption on BAC (Partial loading, Fluidized bed) 1st run

Weight Dry virgin BAC used: 7.02 g				
Cycle	Amount adsorbed (g)	% adsorption capacity (g adsorbed / g adsorbent)	Total heel formed (g)	% accumulated heel formation (g adsorbate remained / g adsorbent)
1	2.17	30.92	0.03	0.38
2	2.16	30.83	0.03	0.44
3	2.16	30.75	0.04	0.53
4	2.17	30.93	0.03	0.47
5	2.18	31.11	0.04	0.57

Table B - 8 Mass balance of 1,2,4 – trimethylbenzene adsorption – desorption on BAC (Partial loading, Fluidized bed) 2nd run

Weight Dry virgin BAC used: 7.00 g				
Cycle	Amount adsorbed (g)	% adsorption capacity (g adsorbed / g adsorbent)	Total heel formed (g)	% accumulated heel formation (g adsorbate remained / g adsorbent)
1	2.08	29.64	-0.01	-0.11
2	2.18	31.13	0.00	0.06
3	2.18	31.18	0.00	-0.07
4	2.17	31.04	0.00	-0.01
5	2.19	31.34	0.00	0.07

Appendix C: Mass balance for adsorption of 500 ppmv VOC mixture on virgin BAC

Table C - 1 Mass balance of VOC mixture adsorption on virgin BAC (Full loading, Fixed bed)

Test No.	Amount of virgin BAC (g)	Amount adsorbed (g)	% adsorption capacity (g adsorbed / g adsorbent)
1	7.00	3.21	45.81
2	8.10	3.91	48.28
3	7.00	3.20	45.79
4	7.00	3.25	46.33

Table C - 2 Mass balance of VOC mixture adsorption on virgin BAC (Full loading, Fluidized bed)

Test No.	Amount of virgin BAC (g)	Amount adsorbed (g)	% adsorption capacity (g adsorbed / g adsorbent)
1	7.00	3.30	47.16
2	7.00	3.55	50.64
3	7.01	3.25	46.31
4	7.01	3.42	48.69
5	7.00	3.50	49.96

Table C - 3 Mass balance of VOC mixture adsorption on virgin BAC (Partial loading, Fixed bed)

Test No.	Amount of virgin BAC (g)	Amount adsorbed (g)	% adsorption capacity (g adsorbed / g adsorbent)
1	7.00	2.19	31.30
2	7.00	2.19	31.33
3	7.00	2.28	32.51
4	7.00	2.39	34.09

Table C - 4 Mass balance of one cycle VOC mixture adsorption on virgin BAC (Partial loading, Fluidized bed)

Test No.	Amount of virgin BAC (g)	Amount adsorbed (g)	% adsorption capacity (g adsorbed / g adsorbent)
1	7.00	2.48	35.40
2	7.00	2.50	35.62
3	7.00	2.47	35.29
4	7.01	1.93	27.52

Appendix D: five cycles of Adsorption – desorption of VOCs’ on BAC

Table D - 1 Mass balance of VOC mixture adsorption – desorption on BAC (Full loading, Fixed bed) 1st run

Weight Dry virgin BAC used: 8.10 g				
Cycle	Amount adsorbed (g)	% adsorption capacity (g adsorbed / g adsorbent)	Total heel formed (g)	% accumulated heel formation (g adsorbate remained / g adsorbent)
1	3.91	48.28	0.30	3.70
2	3.83	47.30	0.51	6.30
3	3.60	44.46	0.69	8.52
4	3.42	42.23	0.80	9.88
5	3.34	41.25	0.87	10.74

Table D - 2 Mass balance of VOC mixture adsorption – desorption on BAC (Full loading, Fixed bed) 2nd run

Weight Dry virgin BAC used: 7.00 g				
Cycle	Amount adsorbed (g)	% adsorption capacity (g adsorbed / g adsorbent)	Total heel formed (g)	% accumulated heel formation (g adsorbate remained / g adsorbent)
1	3.20	45.79	0.24	3.44
2	3.01	42.99	0.35	4.93
3	3.07	43.82	0.52	7.43
4	2.86	40.89	0.67	9.60
5	2.75	39.26	0.74	10.62

Table D - 3 Mass balance of VOC mixture adsorption – desorption on BAC (Full loading, Fixed bed) 3rd run

Weight Dry virgin BAC used: 7.00 g				
Cycle	Amount adsorbed (g)	% adsorption capacity (g adsorbed / g adsorbent)	Total heel formed (g)	% accumulated heel formation (g adsorbate remained / g adsorbent)
1	3.25	46.33	0.22	3.08
2	3.09	44.19	0.39	5.60
3	3.00	42.88	0.52	7.45
4	2.92	41.66	0.66	9.47
5	2.72	38.91	0.76	10.91

Table D - 4 Mass balance of VOC mixture adsorption – desorption on BAC (Full loading, Fluidized bed) 1st run

Weight Dry virgin BAC used: 7.01 g				
Cycle	Amount adsorbed (g)	% adsorption capacity (g adsorbed / g adsorbent)	Total heel formed (g)	% accumulated heel formation (g adsorbate remained / g adsorbent)
1	3.25	46.31	0.23	3.34
2	2.95	42.14	0.25	3.61
3	3.31	47.30	0.36	5.12
4	3.30	47.08	0.49	6.99
5	2.97	42.41	0.52	7.44

Table D - 5 Mass balance of VOC mixture adsorption – desorption on BAC (Full loading, Fluidized bed) 2nd run

Weight Dry virgin BAC used: 7.01 g				
Cycle	Amount adsorbed (g)	% adsorption capacity (g adsorbed / g adsorbent)	Total heel formed (g)	% accumulated heel formation (g adsorbate remained / g adsorbent)
1	3.42	48.69	0.26	3.76
2	3.21	45.79	0.36	5.09
3	3.11	44.30	0.42	5.93
4	3.17	45.14	0.45	6.47
5	3.07	43.77	0.54	7.73

Table D - 6 Mass balance of VOC mixture adsorption – desorption on BAC (Full loading, Fluidized bed) 3rd run

Weight Dry virgin BAC used: 7.00 g				
Cycle	Amount adsorbed (g)	% adsorption capacity (g adsorbed / g adsorbent)	Total heel formed (g)	% accumulated heel formation (g adsorbate remained / g adsorbent)
1	3.50	49.96	0.25	3.63
2	3.33	47.52	0.34	4.80
3	3.22	46.08	0.40	5.76
4	3.17	45.32	0.46	6.57
5	3.13	44.69	0.53	7.52

Table D - 7 Mass balance of VOC mixture adsorption – desorption on BAC (Partial loading, Fixed bed) 1st run

Weight Dry virgin BAC used: 7.00 g				
Cycle	Amount adsorbed (g)	% adsorption capacity (g adsorbed / g adsorbent)	Total heel formed (g)	% accumulated heel formation (g adsorbate remained / g adsorbent)
1	2.28	32.51	0.14	2.03
2	2.23	31.88	0.26	3.73
3	2.19	31.23	0.35	4.97
4	2.17	30.97	0.44	6.34
5	2.18	31.14	0.53	7.57

Table D - 8 Mass balance of VOC mixture adsorption – desorption on BAC (Partial loading, Fixed bed) 2nd run

Weight Dry virgin BAC used: 7.00 g				
Cycle	Amount adsorbed (g)	% adsorption capacity (g adsorbed / g adsorbent)	Total heel formed (g)	% accumulated heel formation (g adsorbate remained / g adsorbent)
1	2.39	34.09	0.15	2.12
2	2.31	33.06	0.27	3.87
3	2.15	30.66	0.39	5.55
4	2.17	31.03	0.45	6.37
5	2.11	30.21	0.52	7.47

Table D - 9 Mass balance of VOC mixture adsorption – desorption on BAC (Partial loading, Fixed bed) 3rd run

Weight Dry virgin BAC used: 7.00 g				
Cycle	Amount adsorbed (g)	% adsorption capacity (g adsorbed / g adsorbent)	Total heel formed (g)	% accumulated heel formation (g adsorbate remained / g adsorbent)
1	2.19	31.33	0.20	2.81
2	1.97	28.17	0.29	4.10
3	1.87	26.71	0.36	5.12
4	1.80	25.68	0.44	6.33
5	1.70	24.32	0.55	7.80

Table D - 10 Mass balance of VOC mixture adsorption – desorption on BAC (Partial loading, Fluidized bed) 1st run

Weight Dry virgin BAC used: 7.01 g				
Cycle	Amount adsorbed (g)	% adsorption capacity (g adsorbed / g adsorbent)	Total heel formed (g)	% accumulated heel formation (g adsorbate remained / g adsorbent)
1	1.93	27.52	0.20	2.80
2	2.14	30.60	0.22	3.15
3	2.41	34.39	0.29	4.18
4	2.21	31.48	0.29	4.12
5	2.23	31.80	0.31	4.39

Table D - 11 Mass balance of VOC mixture adsorption – desorption on BAC (Partial loading, Fluidized bed) 2nd run

Weight Dry virgin BAC used: 7.00 g				
Cycle	Amount adsorbed (g)	% adsorption capacity (g adsorbed / g adsorbent)	Total heel formed (g)	% accumulated heel formation (g adsorbate remained / g adsorbent)
1	2.50	35.62	0.16	2.23
2	2.39	34.12	0.22	3.11
3	2.45	34.98	0.23	3.34
4	2.35	33.57	0.28	4.00
5	2.33	33.27	0.30	4.24

Table D - 12 Mass balance of VOC mixture adsorption – desorption on BAC (Partial loading, Fluidized bed) 3rd run

Weight Dry virgin BAC used: 7.00 g				
Cycle	Amount adsorbed (g)	% adsorption capacity (g adsorbed / g adsorbent)	Total heel formed (g)	% accumulated heel formation (g adsorbate remained / g adsorbent)
1	2.47	35.29	0.11	1.59
2	2.44	34.86	0.19	2.71
3	2.39	34.10	0.24	3.37
4	2.37	33.86	0.28	4.06
5	2.36	33.69	0.31	4.46